subcutaneous tumors in nude mice, and we showed that this was probably due to the amplification of the HSV-*tk* gene copy number and the consequent enhanced spread of the HSV-*tk* product throughout the tumor.

We and others have previously described hybrid vector systems that use adenoviral vectors to deliver retroviral vector and packaging proteins into cells [3–9]. These systems benefit from the efficient gene transfer characteristics of adenoviral vectors along with the stable and long-term gene expression that is typical of retroviral vectors. Initial studies of the co-transduction of adeno-retroviral hybrid vectors showed that transient retrovirus-producing cells can be successfully generated and that these could subsequently cause the transduction of neighboring cells [3,7]. Torrent *et al.* [9] also reported a study with a chimeric vector system that resulted in 10- to 50-fold transgene amplification *in vivo*, although they did not examine the distribution of the transgene or the therapeutic efficacy of their system. In the study reported here, we have altered these hybrid adeno-retroviral vector systems so that the tumor-killing effect of adenovirus-mediated HSV-*tk*/GCV therapy *in situ* is enhanced. Compared with the adenovirus delivery systems that lack retrovirus production, our system provides 89- and 258-fold transgene amplification *in situ* and stronger and wider dispersion of the transgene RNA signal. The enhanced amplification efficiency is most likely due to the *in situ* generated progeny retrovirus particles bearing the VSV-G envelope protein, which has a broader host range and higher transduction efficiency than murine leukemia virus derived retrovirus [7]. Murine leukemia virus derived retroviral vectors have had limited application in gene therapy because of low transduction efficiency of tissues, both *in vitro* and *in vivo*. One study showed that the transduction efficiency of the amphotropic vector into human cancer cells was not dose-dependent and reached a plateau or even decreased, especially at high MOIs [25]. This may be attributed in part to the presence of the envelope protein and non-infectious particles that compete for the receptor of infectious amphotropic viruses. In contrast, the receptor for VSV-G exists in abundance on the cell surface. Thus, our hybrid vector system pseudotyped with the VSV-G envelope glycoprotein is an alternative tool for efficient transduction.

For safety reasons, the retroviral functions in our system were split into different adenoviral backbones. However, there are some reports of studies that use a single helper-dependent adenovirus (HDAd) vector to accommodate large inserts. A vector system that uses an HDAd vector as a carrier to deliver a replication-competent ecotropic retrovirus vector has been developed [26]. An adenovirus/lentivirus hybrid vector on a single HDAd backbone was also developed for stable integration [27]. Although adenovirus-mediated transduction seems to be efficient in most cancers, there are several reports of studies using different viral components that convert tumor cells into retroviral producer cells. One of these employs a single-step system with herpes simplex virus/Epstein-Barr virus hybrid amplicons that converts cells into retrovirus vector producers [28]. Infection of primary gliomas with this system resulted in the production of retrovirus vectors and long-term retention *in vitro*. Poxviral/retroviral chimeric vectors also allow cytoplasmic production of defective retroviral particles [29]. Vaccinia-mediated expression of retroviral vector particles could be observed as early as 3 h post-infection and resulted in the stable transduction of NIH/3T3 cells. An alphavirus/retrovirus hybrid vector has also been used to transduce the retroviral vector packaging cell line [30]. The produced factor IX minigene-containing retroviral vectors were used for stable transduction *in vitro*.

When we used our hybrid vector system to treat a subcutaneous tumor model, we detected enhanced transgene expression together with an increased therapeutic effect *in vivo*. This suggests that the retroviral progeny are efficiently produced *in situ*. Although the efficacy of this system has to be evaluated in orthotopic models, current observations suggest that it is a promising method that has many possible applications in cancer gene therapy.

Acknowledgements

We wish to thank Dr. Tom Shenk for providing dl327 and Drs. Hiroshi Amanuma and Kiyotake Tobita for their support. We also wish to thank Ms. Miyoko Mitsu and Dr. Masahide Koremoto for their technical support and encouragement. This work was supported in part by Grants-in-Aid for Scientific Research from the Ministry of Education, Culture, Sports, Science and Technology of Japan, by the Jichi Medical School young investigator award, by the Uehara Memorial Foundation, by the Osaka Cancer Research Foundation, and by the Nakajima Foundation.

References

1. Ram Z, Culver KW, Oshiro EM, *et al.* Therapy of malignant brain tumors by intratumoral implantation of retroviral vector-producing cells. *Nat Med* 1997; 3: 1354–1361.
2. Rainov NG. A phase III clinical evaluation of herpes simplex virus type 1 thymidine kinase and ganciclovir gene therapy as an adjuvant to surgical resection and radiation in adults with previously untreated glioblastoma multiforme. *Hum Gene Ther* 2000; **11**: 2389–2401.
3. Feng M, Jackson WH Jr, Goldman CK, *et al.* Stable in vivo gene transduction via a novel adenoviral/retroviral chimeric vector. *Nat Biotechnol* 1997; **15**: 866–870.
4. Bilbao G, Feng M, Rancourt C, Jackson WJ, Curiel DT. Adenoviral/retroviral vector chimeras: a novel strategy to achieve high-efficiency stable transduction in vivo. *FASEB J* 1997; **11**: 624–634.
5. Ramsey WJ, Caplen NJ, Li Q, Higginbotham JN, Shah M, Blaese RM. Adenovirus vectors as transcomplementing templates for the production of replication defective retroviral vectors. *Biochem Biophys Res Commun* 1998; **246**: 912–919.
6. Lin X. Construction of new retroviral producer cells from adenoviral and retroviral vectors. *Gene Ther* 1998; **5**: 1251–1258.
7. Caplen NJ, Higginbotham JN, Scheel JR, *et al.* Adeno-retroviral chimeric viruses as in vivo transducing agents. *Gene Ther* 1999; 6: 454–459.
8. Duisit G, Salvetti A, Moullier P, Cosset FL. Functional characterization of adenoviral/retroviral chimeric vectors and their use for efficient screening of retroviral producer cell lines. *Hum Gene Ther* 1999; 10: 189–200.

9. Torrent C, Jullien C, Klatzmann D, Perricaudet M, Yeh P. Transgene amplification and persistence after delivery of retroviral vector and packaging functions with E1/E4-deleted adenoviruses. *Cancer Gene Ther* 2000; **7**: 1135–1144.
10. Okada T, Ramsey J, Munir J, Wildner O, Blaese M. Efficient directional cloning of recombinant adenovirus vectors using DNA-protein complex. *Nucleic Acids Res.* 1998; **26**: 1947–1950.
11. Treisman J, Hwu P, Minamoto S, *et al.* Interleukin-2-transduced lymphocytes grow in an autocrine fashion and remain responsive to antigen. *Blood* 1995; **85**: 139–145.
12. Okada T, Shah M, Higginbotham JN, *et al.* AV.TK-mediated killing of subcutaneous tumors in situ results in effective immunization against established secondary intracranial tumor deposits. *Gene Ther* 2001; **8**: 1315–1322.
13. Stein R, Ziff EB. HeLa cell beta-tubulin gene transcription is stimulated by adenovirus 5 in parallel with viral early genes by an E1a-dependent mechanism. *Mol Cell Biol* 1984; **4**: 2792–2801.
14. Graham FL, Prevec L. Adenovirus-based expression vectors and recombinant vaccines. *Biotechnology* 1992; **20**: 363–390.
15. Yoshida Y, Emi N, Hamada H. VSV-G-pseudotyped retroviral packaging through adenovirus-mediated inducible gene expression. *Biochem Biophys Res Commun* 1997; **232**: 379–382.
16. Cosset FL, Takeuchi Y, Battini JL, Weiss RA, Collins MK. High-titer packaging cells producing recombinant retroviruses resistant to human serum. *J Virol* 1995; **69**: 7430–7436.
17. Benda P, Someda K, Messer J, Sweet WH. Morphological and immunochemical studies of rat glial tumors and clonal strains propagated in culture. *J Neurosurg* 1971; **34**: 310–323.
18. Bethea JR, Gillespie GY, Chung IY, Benveniste EN. Tumor necrosis factor production and receptor expression by a human malignant glioma cell line, D54-MG. *J Neuroimmunol* 1990; **30**: 1–13.
19. Graham FL, Smiley J, Russell WC, Nairn R. Characteristics of a human cell line transformed by DNA from human adenovirus type 5. *J Gen Virol* 1977; **36**: 59–74.
20. Wildner O, Candotti F, Krecko EG, Xanthopoulos KG, Ramsey WJ, Blaese RM. Generation of a conditionally neo(r)-containing retroviral producer cell line: effects of neo(r) on retroviral titer and transgene expression. *Gene Ther* 1998; **5**: 684–691.
21. Wigler M, Pellicer A, Silverstein S, Axel R. Biochemical transfer of single-copy eucaryotic genes using total cellular DNA as donor. *Cell* 1978; **14**: 725–731.
22. Onodera M, Yachie A, Nelson DM, Welchlin H, Morgan RA, Blaese RM. A simple and reliable method for screening retroviral producer clones without selectable markers. *Hum Gene Ther* 1997; **8**: 1189–1194.
23. Onodera M, Nelson DM, Yachie A, *et al.* Development of improved adenosine deaminase retroviral vectors. *J Virol* 1998; **72**: 1769–1774.
24. Harstrick A, Casper J, Guba R, Wilke H, Poliwoda H, Schmoll HJ. Comparison of the antitumor activity of cisplatin, carboplatin, and iproplatin against established human testicular cancer cell lines in vivo and in vitro. *Cancer* 1989; **63**: 1079–1083.
25. Arai T, Takada M, Ui M, Iba H. Dose-dependent transduction of vesicular stomatitis virus G protein-pseudotyped retrovirus vector into human solid tumor cell lines and murine fibroblasts. *Virology* 1999; **260**: 109–115.
26. Soifer H, Higo C, Logg CR, *et al.* A novel, helper-dependent, adenovirus-retrovirus hybrid vector: stable transduction by a two-stage mechanism. *Mol Ther* 2002; **5**: 599–608.
27. Kubo S, Mitani K. A new hybrid system capable of efficient lentiviral vector production and stable gene transfer mediated by a single helper-dependent adenoviral vector. *J Virol* 2003; **77**: 2964–2971.
28. Sena-Esteves M, Saeki Y, Camp SM, Chiocca EA, Breakefield XO. Single-step conversion of cells to retrovirus vector producers with herpes simplex virus-Epstein-Barr virus hybrid amplicons. *J Virol* 1999; **73**: 10 426–10 439.
29. Holzer GW, Mayrhofer JA, Gritschenberger W, Dorner F, Falkner FG. Poxviral/retroviral chimeric vectors allow cytoplasmic production of transducing defective retroviral particles. *Virology* 1999; **253**: 107–114.
30. Wahlfors JJ, Morgan RA. Production of minigene-containing retroviral vectors using an alphavirus/retrovirus hybrid vector system. *Hum Gene Ther* 1999; **10**: 1197–1206.

Neurobiology of Disease

Presynaptic Localization of Neprilysin Contributes to Efficient Clearance of Amyloid-β Peptide in Mouse Brain

Nobuhisa Iwata,[1] Hiroaki Mizukami,[2] Keiro Shirotani,[1] Yoshie Takaki,[1] Shin-ichi Muramatsu,[3] Bao Lu,[4] Norma P. Gerard,[4] Craig Gerard,[4] Keiya Ozawa,[2] and Takaomi C. Saido[1]

[1]Laboratory for Proteolytic Neuroscience, RIKEN Brain Science Institute, Wako-shi, Saitama 351-0198, Japan, [2]Division of Genetic Therapeutics, Center for Molecular Medicine, and [3]Division of Neurology, Department of Medicine, Jichi Medical School, Tochigi 329-0498, Japan, and [4]Department of Pediatrics and Medicine, Harvard Medical School, Boston, Massachusetts 02115

A local increase in amyloid-β peptide (Aβ) is closely associated with synaptic dysfunction in the brain in Alzheimer's disease. Here, we report on the catabolic mechanism of Aβ at the presynaptic sites. Neprilysin, an Aβ-degrading enzyme, expressed by recombinant adeno-associated viral vector-mediated gene transfer, was axonally transported to presynaptic sites through afferent projections of neuronal circuits. This gene transfer abolished the increase in Aβ levels in the hippocampal formations of neprilysin-deficient mice and also reduced the increase in young mutant amyloid precursor protein transgenic mice. In the latter case, Aβ levels in the hippocampal formation contralateral to the vector-injected side were also significantly reduced as a result of transport of neprilysin from the ipsilateral side, and in both sides soluble Aβ was degraded more efficiently than insoluble Aβ. Furthermore, amyloid deposition in aged mutant amyloid precursor protein transgenic mice was remarkably decelerated. Thus, presynaptic neprilysin has been demonstrated to degrade Aβ efficiently and to retard development of amyloid pathology.

Key words: Alzheimer; axonal transport; axoplasmic transport; gene; hippocampus; presynaptic; projection; endopeptidase; amyloid-β peptide; gene transfer; adeno-associated viral vector; degradation; perforant path

Introduction

Alzheimer's disease (AD) is characterized by extracellular deposition of amyloid-β peptide (Aβ), intracellular neurofibrillary tangles, and synaptic and neuronal loss (Hardy and Selkoe, 2002). Aβ deposition is a triggering event that causes a long-term pathological cascade of AD and is closely associated with the metabolic balance between Aβ anabolic and catabolic activities (Hardy and Selkoe, 2002; Saido, 2003; Saido and Nakahara, 2003). As almost all familial AD mutations cause an increase in the anabolism of a particular form of Aβ, $Aβ_{1-42}$, leading to Aβ deposition and accelerating AD pathology, a chronic reduction in the catabolic activity would also promote Aβ deposition (Hardy and Selkoe, 2002; Saido, 2003; Saido and Nakahara, 2003). Neprilysin (EC 3.4.24.11), previously called neutral endopeptidase-24.11, enkephalinase, or NEP, is a rate-limiting peptidase participating in Aβ catabolism, as proven by *in vivo* experiments tracing the catabolism of radiolabeled Aβ in brain and by reverse genetics studies (Iwata et al., 2000, 2001). Neprilysin-specific inhibitors and neprilysin gene disruption in mice abolished this function. Neprilysin gene disruption caused a gene dosage-dependent elevation of the endogenous Aβ levels in the mouse brain, suggesting that even a subtle reduction of neprilysin activity will contribute to AD development by promoting Aβ deposition (Iwata et al., 2001). This conclusion was reinforced by the observation that expression levels of neprilysin were particularly low in regions vulnerable to senile plaque development, such as hippocampus and midtemporal gyrus (Yasojima et al., 2001a,b). The neprilysin levels in these regions were selectively reduced by ~50% in sporadic AD patients, compared with age-matched controls. In addition, in normal aging of laboratory mice, neprilysin levels were selectively decreased at the outer molecular layer of the dentate gyrus and the stratum lucidum, the terminal zones of the lateral perforant path (Iwata et al., 2002), which are highly vulnerable regions to AD pathology (Gomez-Isla et al., 1996). Thus, age-related decline of neprilysin activity in these specific regions is likely to promote the pathogenesis of sporadic AD.

Much attention has been directed to a possible role of Aβ in synaptic dysfunction observed in brains of AD patients and several lines of mutant amyloid precursor protein (APP) transgenic mice (Hartley et al., 1999; Hsia et al., 1999; Lue et al., 1999; Mucke et al., 2000; Buttini et al., 2002; Walsh et al., 2002; Wang et al., 2002). An aberrant increase in Aβ at presynaptic sites has been suggested to give rise to synaptic dysfunction (Terry et al., 1991; Sze et al., 1997; Selkoe, 2002). Aβ generated from axonally transported APP is released from presynaptic sites and contributes to

Received Oct. 24, 2003; revised Dec. 2, 2003; accepted Dec. 7, 2003.

This work was supported by a research grant from RIKEN BSI and a Grant-in-Aid for Scientific Research (B) from the Japan Society for the Promotion of Science. We thank Misaki Sekiguchi, Yukio Matsuba, Kaori Watanabe, and Emi Hosoki for technical assistance, and Dr. Makoto Higuchi for helpful discussions. We also thank Takeda Chemical Industries, Ltd., Dr. John A Chiorini (National Institute of Dental and Craniofacial Research, National Institutes of Health), and Dr. Karen Hsiao-Ashe (Department of Neurology, University of Minnesota) for kindly providing anti-Aβ monoclonal antibodies for sandwich ELISA, the AAVS vector production system, and Tg2576 mice, respectively.

Correspondence should be addressed to Nobuhisa Iwata at the above address. E-mail: iwatan@brain.riken.jp.

K. Shirotani's present address: Laboratory for Alzheimer's and Parkinson's Disease, Department of Biochemistry, Adolf-Butenandt-Institute, Ludwig-Maximilians-University, D-80336 Munich, Germany.

DOI:10.1523/JNEUROSCI.4792-03.2004

 0270-6474/04/240991-08$15.00/0

extracellular amyloid deposition (Buxbaum et al., 1998; Lazarov et al., 2002; Sheng et al., 2002). However, much less is known about the catabolic mechanism of Aβ at the presynaptic sites. Neprilysin was mainly detected in presynapses and on or around axons in the hippocampal formation by double immunostaining with presynaptic and axonal marker proteins (Fukami et al., 2002) and by subcellular fractionation and electron microscopic immunocytochemistry (Barnes et al., 1988, 1992), leading us to the notion that neprilysin regulates Aβ concentration around presynaptic sites and that a reduction of neprilysin activity may elicit local elevation of Aβ concentration in the extracellular space close to synapses, possibly affecting the local pathology during the course of AD development.

In the present study, we attempted to express neprilysin in the hippocampal formation of mice *in vivo* by means of viral vector-mediated gene transfer to confirm the pathological significance of presynaptic neprilysin. For this purpose, we selected a recombinant adeno-associated virus (rAAV) vector, because it offers the advantages of the ability to infect nondividing cells, affording a non-pathogenic, long-term transgene expression without a substantial inflammatory response (Okada et al., 2002). Because inflammatory responses diversely affect clearance of the amyloid burden (Weninger and Yankner, 2001), it is important to avoid inducing such a response to viral infection to elucidate properly the effect of neprilysin gene transfer. In addition, we used expression of an inactivated form of neprilysin as a negative control. Recently, Marr et al. (2003) reported successful reduction of Aβ by neprilysin gene transfer with a lentiviral vector to the brain of mutant APP transgenic mice, in which immunoreactive neprilysin was detected in cell bodies in most cases. However, the significance of Aβ degradation by neprilysin at the presynaptic sites remains unclear. Here, we show that neprilysin expressed in the neurons was axonally transported to presynaptic sites and presynaptic neprilysin efficiently degraded Aβ, eventually decelerating Aβ deposition.

Materials and Methods

Recombinant AAV vector production. The AAV vector plasmid contains human neprilysin cDNA or its mutant (inactivated form) at the C terminus of the human cytomegalovirus immediate-early promoter and the human growth hormone first intron at the N terminus of the simian virus 40 polyadenylation signal sequence between the inverted terminal repeats of the AAV serotype 5 genome (Chiorini et al., 1999). rAAV5 vectors were produced with AAV vector plasmid and AAV helper plasmids encoding rep and cap sequences from AAV serotype 5 and pHelper plasmid from the AAV Helper-Free System (Stratagene, La Jolla, CA). In brief, subconfluent human embryonic kidney 293 cells were transiently transfected by the calcium phosphate method. Seventy-two hours after transfection, the cells were collected and subjected to three cycles of freeze–thaw lysis. rAAV vectors were purified on two sequential continuous cesium chloride density gradients, and the final particle titer was estimated by quantitative DNA dot-blot hybridization. Before administration, rAAV vectors were diluted in HEPES-buffered saline to 0.1–2.0 × 10^{10} genome copies/0.6 μl.

Animals and surgical procedure. All animal experiments were performed in compliance with the institutional guidelines. Wild-type, neprilysin-deficient (Lu et al., 1995), young and aged Tg2576 (Hsiao et al., 1996) mice in littermates were evenly assigned to rAAV-NEP vector-injected group and three negative control groups that were injected with rAAV-NEPinactive vector, rAAV-*LacZ* vector, and the vehicle, respectively. A 26 S gauge needle equipped with a 1.0 μl motorized Hamilton syringe was inserted into the dentate gyrus (stereotaxic coordinates: anteroposterior, 2.4 mm; mediolateral, 2.0 mm; dorsoventral, 2.1 mm), the frontal isocortex (−2.3, 2.0, 1.5 mm), or the lateral entorhinal cortex (4.1, 4.5, 2.3 mm) of anesthetized mice. Two minutes after the insertion, 0.6 μl of a virus solution or vehicle was injected at a constant flow rate of 0.06 μl/min, and the needle was left in this configuration for an additional 2 min, to prevent reflux of the injected material along the injection track, before being slowly retracted.

Immunohistochemistry. The mouse brain was fixed by a transcardial perfusion with phosphate-buffered 4% paraformaldehyde and then embedded in paraffin. Four-micrometer-thick sections were mounted onto aminopropyltriethoxysilane-coated glass slides. Immunostaining for neprilysin was performed using the high-temperature antigen unmasking technique and the fluorescence-indirect tyramide signal amplification (TSA) method and anti-neprilysin monoclonal antibody (56C6; 1:200 dilution, Novocastra, Newcastle, UK) according to our previous report (Fukami et al., 2002). The immunostaining for β-galactosidase was performed using anti-β-galactosidase antibody (AB1211; 1:1500 dilution; Chemicon, Temecula, CA). Sections were observed under an Axiophot 2 fluorescence microscope (Zeiss, Göttingen, Germany), and the digital images were captured with a 2.5× objective and a CCD camera (ORCA-ERII; Hamamatsu Photonics KK, Shizuoka, Japan) using image analysis software, MetaMorph, version 6.1 (Universal Imaging Corporation, Downington, PA).

Multiple immunofluorescence staining of neprilysin and marker proteins, SV2A (119002; 1:500 dilution; Synaptic Systems, Göttingen, Germany), tau (Tau1; 1:200 dilution; Chemicon), MAP2 (M121; 1:10 dilution; Leinco Technologies, Manchester, UK), or GFAP (L1812; prediluted; Dako, Carpinteria, CA) was performed as described previously (Fukami et al., 2002). When we used anti-GAP43 (AB5220; 1:2000 dilution; Chemicon), anti-SNAP-25 (SC7538; 1:25 dilution; Santa Cruz, CA), anti-GluR1 (AB1504; 1:400 dilution; Chemicon), or anti-Aβ antibody, which recognizes the C-terminal of Aβ42 (C42) (Saido et al., 1995), we used a fluorescence-direct TSA method combined with horseradish peroxidase-labeled dextran polymer-conjugated goat anti-rabbit IgG (Envision plus; Dako) (Fukami et al., 2002). The sections labeled with immunofluorescence were observed under an IX70 inverted microscope incorporating a confocal laser scanning system FV300 with argon, helium–neon (G) and helium–neon (R) lasers (Olympus Optical Co., Tokyo, Japan). FITC/Alexa 488, Texas Red, and Alexa 633 were excited with 488, 543, and 633 nm laser beams and observed through 510–530, 560–600, and 660 nm bandpass emission filters, respectively. All of the single images were acquired by a triple scan with Fluoview, version 4.2 software (Olympus Optical) using a 100× oil immersion objective, then merged and saved as digitized tagged-image format files to retain maximum resolution.

Quantitative assessment of Aβ deposition. Three months after unilateral injection of rAAV-NEPinactive or rAAV-NEP (1.3 × 10^{10} genome copies) into the hippocampal formation of 18-month-old Tg2576 mice, the brain sections were immunostained using anti-Aβ antibody C42 and visualized by the avidin–biotin–peroxidase complex procedure (Vectastain ABC kits; Vector Laboratories, Burlingame, CA) using 3,3-diaminobenzidine as a chromogen. Sections were observed with a light microscope, Provis AX80 (Olympus Optical), using a 4× objective and a 1.5× digital zoom, and digital images were captured with a DP70 digital microscope camera (Olympus Optical). Densities of immunoreactive Aβ deposits in various areas of the hippocampal formation and cerebral cortex were measured using MetaMorph by an investigator "blinded" to sample identity, after the raw images had been inverted using image-editing software (Adobe Photoshop 7.0; Adobe Systems, Inc., Mountain View, CA). To reduce the variance among tissue sections, we used the average of data from three sections per mouse as an individual value.

Assay of neprilysin-dependent neutral endopeptidase activity. Triton X-100-solubilized membrane fractions from hippocampal formations and cerebral cortices of intact, buffer-, or rAAV-vector-injected mice were prepared to assay neutral endopeptidase activity as described previously (Iwata et al., 2002). The neprilysin-dependent neutral endopeptidase activity was fluorometrically assayed using 0.1 mM succinyl-Ala-Ala-Phe-MCA (Bachem, Bubendorf, Switzerland) as a substrate and determined from the fluorescence intensity (excitation, 390 nm; emission, 460 nm), based on the decrease in the rate of digestion caused by 10 μM thiorphan, a specific inhibitor of neprilysin. Protein concentrations were determined using a BCA protein assay kit (Pierce, Rockford, IL).

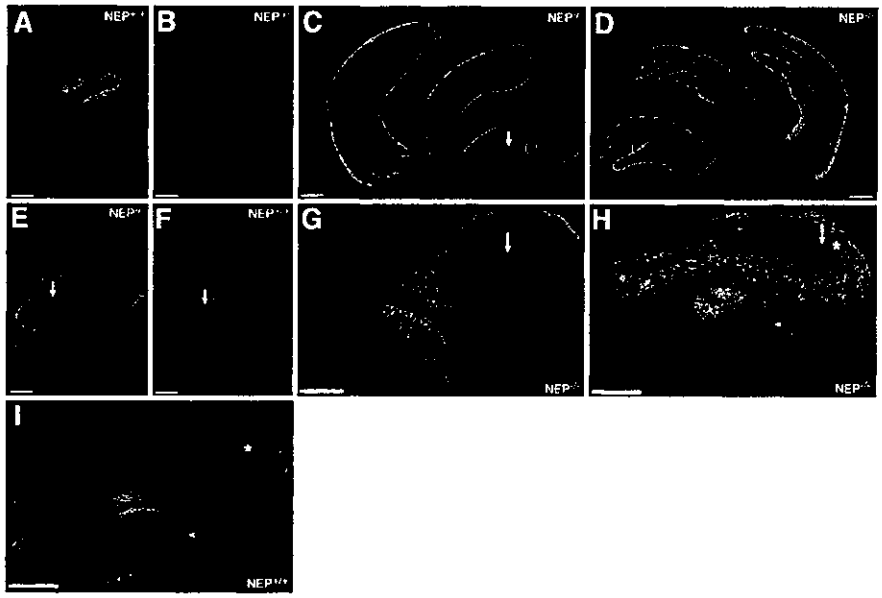

Figure 1. Expression profiles of neprilysin in brain after the vector injection. Immunohistochemical staining for neprilysin (*A–E,G–I*) or β-galactosidase (*F*) was performed 4 weeks after the injection of rAAV vectors (1.3×10^{10} genome copies). rAAV-NEP (*C*) or rAAV-NEPinactive (*E*) was unilaterally injected into the dentate gyrus of *neprilysin* $^{-/-}$ mouse. *C, E,* and *F* show the injection (ipsilateral) sides; *D* is the contralateral side to *C*. Three immunostained sections from anterior to posterior are shown in *C* and *D*. *F* shows the expression pattern of β-galactosidase in the dentate gyrus of wild-type mouse injected with rAAV-*LacZ*. *A, I,* and *B* show typical immunostaining patterns for *neprilysin* $^{+/+}$ and *neprilysin* $^{-/-}$ mouse brains, respectively. rAAV-NEP was injected into the frontal isocortex (*G*) and lateral entorhinal cortex (*H*) of *neprilysin* $^{-/-}$ mice. Arrows, arrowheads, and asterisks indicate the injection sites, the outer molecular layer of the dentate gyrus, and the lateral entorhinal cortex, respectively. Boxed areas were analyzed for subcellular localization of neprilysin as shown in Figure 2. Scale bars, 500 μm.

Aβ quantitation. The hippocampal formations and cerebral cortices were homogenized in 50 mM Tris-HCl buffer, pH 7.6, containing 150 mM NaCl and the protease inhibitor cocktail (TBS) with a Teflon-glass homogenizer and centrifuged at 200,000 × *g* for 20 min at 4°C. The supernatant was defined as the soluble (TBS-extractable) fraction, and guanidine–HCl was added to give 0.5 M (final concentration) before application to ELISA. The pellet was solubilized by sonication in 6 M guanidine–HCl buffer containing the protease inhibitor cocktail. The solubilized pellet was centrifuged at 200,000 × *g* for 20 min at 4°C, after which the supernatant was diluted 12 times to reduce the concentration of guanidine–HCl and used as the insoluble fraction. The amounts of $A\beta_{X\text{-}40}$ and $A\beta_{X\text{-}42}$ in each fraction were determined by sandwich ELISA using monoclonal antibodies BNT77/BA27 and BNT77/BC05, respectively.

Statistical analysis. All data were expressed as means ± SEM. For comparisons of the means between two groups, statistical analysis was performed by applying Student's *t* test after confirming equality between the variances of the groups. If the variances were unequal, Mann–Whitney *U* tests were performed (StatView 5.0 software; SAS, Cary, NC). Comparisons of the means among more than three groups were done by a one-way ANOVA followed by Dunnett's multiple-range test (StatView 5.0 software). *P* values of <0.05 were considered to be significant.

Results

Expression profiles of neprilysin in the brain after rAAV-mediated gene transfer

To evaluate the expression pattern of neprilysin, we injected an rAAV vector into the brain of neprilysin-deficient mouse and examined the expression profile by means of specific immunochemical staining for neprilysin. This staining gave specific signals of endogenous neprilysin in wild-type mice, but not in neprilysin-deficient mice (Fig. 1*A,B*). Expression of neprilysin after a single injection of rAAV-NEP vector into the unilateral dentate gyrus was spread over the bilateral hippocampal formations in the neprilysin-null background (Fig. 1*C,D*). The localization of neprilysin in the contralateral side of the hippocampal formation was similar to the pattern of afferent projection from the ipsilateral neurons, that is, the commissural, associational, and associational/commissural projections (Amaral and Witter, 1995). Intrahippocampally, intense signals of immunoreactive neprilysin were detected at the stratum lucidum (the projection site from the granular cells of the dentate gyrus) of the ipsilateral side 1 week after rAAV-NEP vector injection (data not shown), although they could not be clearly seen at 4 weeks after injection because of the more intense signal over the entire hippocampal formation (Fig. 1*C*). The inactivated form of neprilysin, one of the negative control proteins, was expressed to a similar extent and with a similar spatial pattern to that of wild-type neprilysin after rAAV vector-mediated gene-transfer (Fig. 1*E*). The expression of β-galactosidase, another negative control protein, was almost wholly restricted to the injection site, and its subcellular localization was limited to the neuronal somas (Fig. 1*F*), in contrast to neprilysin. The apparent difference of gene expression level of β-galactosidase can be simply explained in terms of the detection sensitivity of immunostaining, but the difference of distribution appears to be attributable to the nature of the expressed protein.

Expression of neprilysin was also detected after injections of rAAV-NEP vector into isocortex (Fig. 1*G*) and allocortex (Fig. 1*H*) regions, such as the entorhinal cortex. In particular, localization of neprilysin after the injection of rAAV-NEP vector into the lateral entorhinal cortex was observed in the outer molecular layer of the dentate gyrus, which is consistent with the projection of the perforant path. This distribution pattern of neprilysin was observed in intact wild-type mice (Fig. 1*I*). Taken together with the findings in the case of hippocampal rAAV-NEP injections, this result indicates that neprilysin expressed after the injection of rAAV-NEP vectors can be transported through appropriate projection pathways, as would be required for a widespread presynaptic distribution of exogenous neprilysin.

Next, we examined the subcellular localization of neprilysin in the contralateral hippocampal formation by confocal double immunostaining for neprilysin and several marker proteins, after the injection of the rAAV-NEP vector into the hippocampal formation of neprilysin-deficient mice. Neprilysin was well colocalized with presynaptic markers, SV2A (Fig. 2*A*), GAP43 (Fig. 2*B*), and SNAP-25 (data not shown), and also with an axonal marker tau (Fig. 2*C*), but not with a somatodendritic marker MAP2, a postsynaptic marker GluR1, or an astrocytic marker GFAP (Fig. 2*D–F*), in agreement with the colocalization patterns of neprilysin observed in the brain of intact wild-type mice (Fukami et al., 2002). Similarly, neprilysin observed at the ipsilateral hippocampal formation was present at the presynaptic terminals in various intrahippocampal circuits, but not in somatodendritic areas or astrocytes (data not shown). These results demonstrate that rAAV-NEP-derived neprilysin is axonally transported to the pre-

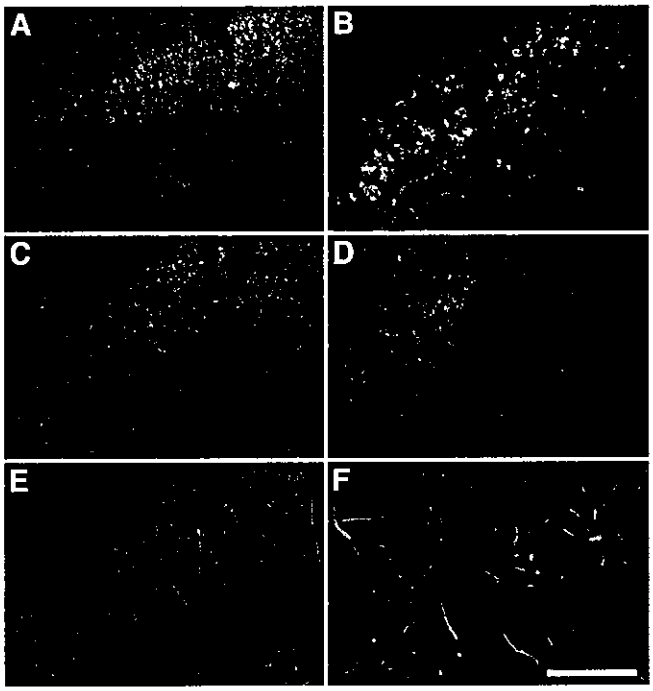

Figure 2. Subcellular localization of neprilysin expressed in the hippocampal formation after gene transfer. The subcellular localization of neprilysin expressed in the dentate gyrus of the contralateral hippocampal formation of *neprilysin* $^{-/-}$ mice by rAAV-mediated gene transfer was analyzed by double immunofluorescence staining for neprilysin (red) and several marker proteins (green). The merged images are shown here. *A*, SV2; *B*, GAP-43; *C*, tau; *D*, GluR1; *E*, MAP2; *F*, GFAP. Scale bar, 20 μm.

synaptic terminals that are supposed to be primary sites of Aβ catabolism, as expected from the fact that neprilysin is a type II membrane-associated protein.

Functional expression of neprilysin

We next investigated the levels of neprilysin gene expression by the measurement of neprilysin activity. One week after the single injection of rAAV-NEP vector into the hippocampal formation of neprilysin-deficient mice, the neprilysin activity was increased in a vector-dose-dependent manner, while the activity in the buffer- or rAAV-NEPinactive-injected group remained at the level observed in intact neprilysin-deficient mice (Fig. 3*A*). The injection of rAAV-NEP vector into the wild-type mice increased neprilysin activity over that in the intact or buffer-injected group to a degree which was similar to that in neprilysin-deficient mice injected with the equivalent amount of rAAV-NEP vector (Fig. 3*A*). In a time course experiment, the expression of neprilysin (based on activity measurement) was increased by a maximum of tenfold at 16 weeks after the infection, compared with the rAAV-NEPinactive-injected group, and continued to be increased up to 24 weeks (Fig. 3*B*).

Rescue of neprilysin-deficient mice from Aβ accumulation

We investigated changes in Aβ levels in both soluble (TBS-extractable) and insoluble (GuHCl-extractable) fractions extracted from hippocampal formations 4 weeks after bilateral injection of either rAAV vectors or buffer into the hippocampal formations of 10-week-old neprilysin-deficient mice (Fig. 4*A*). The Aβ levels in both fractions of intact neprilysin-deficient mice were increased up to approximately twofold, compared with those of wild-type mice, as reported previously (Iwata et al., 2001). After the injection of buffer, rAAV-*LacZ* vector, or rAAV-

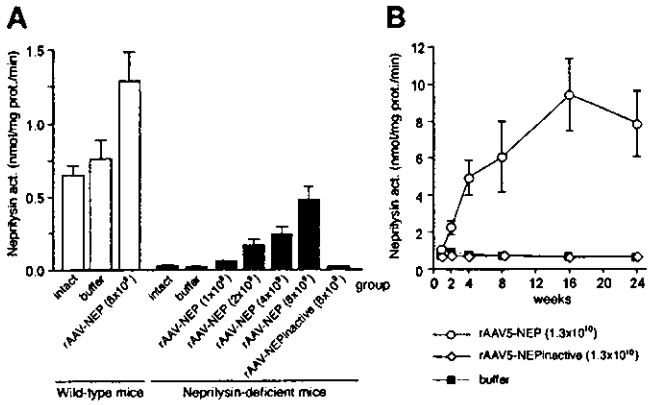

Figure 3. Functional expression of neprilysin after gene transfer. *A*, Levels of neprilysin-dependent endopeptidase activities in ipsilateral hippocampal formations of intact, buffer-injected, rAAV-NEP-injected, or rAAV-NEPinactive-injected *neprilysin* $^{+/+}$ and *neprilysin* $^{-/-}$ mice. Each column with a bar represents the mean ± SE of three mice. *B*, Duration of neprilysin gene expression. The endopeptidase activities in ipsilateral hippocampal formations were measured 1, 2, 4, 8, 16, and 24 weeks after unilateral injection of rAAV-NEP, rAAV-NEPinactive, or buffer into the hippocampal formation of *neprilysin* $^{+/+}$ mice. Each column with a bar represents the mean ± SE of three mice.

NEPinactive vector into neprilysin-deficient mice, the Aβ levels in each fraction remained unchanged, but the injection of rAAV-NEP vector significantly decreased Aβ to the wild-type levels, thus almost completely abolishing the increase of Aβ levels induced by neprilysin deficiency. In the experiments using wild-type mice, the neprilysin gene transfer further decreased the $Aβ_{x-40}$ levels in both fractions (Fig. 4*B*). Although we examined $Aβ_{x-42}$ levels, most of the values were below the reliable determination range of the standard curve in ELISA (data not shown).

Efficient degradation of Aβ by presynaptic neprilysin

In the Aβ measurement shown in Figure 4, we analyzed the hippocampal formations of both sides after bilateral injections of rAAV5 vectors or buffer, because the use of unilateral injection did not provide reliable data. However, this did not allow us to clarify the effect of exogenous neprilysin that was axonally transported to the presynaptic terminals. Therefore, we investigated mutant APP transgenic (Tg2576) (Hsiao et al., 1996) mice after the unilateral injection of rAAV5-NEP vector to demonstrate the significance of axonal transport and presynaptic localization of neprilysin for efficient Aβ degradation. Eight weeks after a unilateral injection of rAAV-NEP vector, the Aβ levels in the ipsilateral hippocampal formation of Tg2576 mice were significantly reduced, particularly in the soluble fraction (50 and 40% reduction for $Aβ_{x-40}$ and $Aβ_{x-42}$, respectively) (Fig. 5*A*), compared with those after injection of rAAV-NEPinactive. In the contralateral hippocampal formation (Fig. 5*B*), Aβ levels in the soluble fraction were reduced to a comparable level to the ipsilateral side (33 and 28% reduction for $Aβ_{x-40}$ and $Aβ_{x-42}$, respectively), although the increase in neprilysin activity in the rAAV-NEP-injected group was 2.6-fold and much lower than the increase in the ipsilateral side, which amounted to 20-fold relative to the negative controls (Fig. 5*C*). This result suggests that a small increase in neprilysin activity, as observed at the contralateral side, may be enough for substantial removal of soluble Aβ. The Aβ levels and neprilysin activities of the rAAV-NEPinactive group remained unchanged between the ipsilateral and the contralateral sides (Fig. 5*A*,*B*). In addition, we observed no marked change in either Aβ levels or neprilysin activity in the cerebral cortices of both sides, to which no exogenous neprilysin or its mutant was found

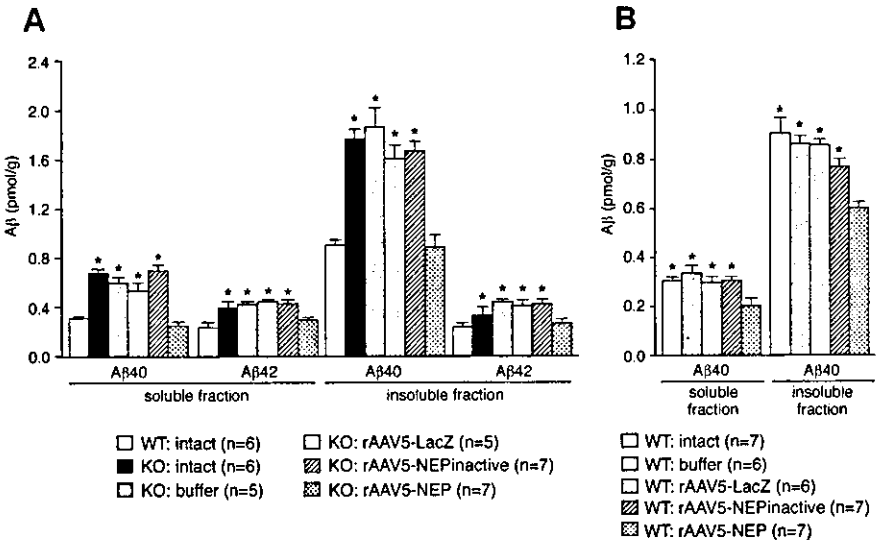

Figure 4. Reduction in intrahippocampal Aβ levels in neprilysin-deficient and wild-type mice after gene transfer. *A*, Aβ levels in both soluble and insoluble fractions of bilateral hippocampal formations were determined by sandwich ELISA 4 weeks after bilateral injection of rAAV-*LacZ* (1.3×10^{10} genome copies), rAAV-NEPinactive (1.3×10^{10}), rAAV-NEP (1.3×10^{10}), or buffer into the hippocampal formations of 10-week-old *neprilysin* $^{-/-}$ mice. Each column with a bar represents the mean ± SE of 5–7 mice. *B*, $A\beta_{x\text{-}40}$ levels were determined 4 weeks after bilateral injection of rAAV vectors or buffer into the hippocampal formations of 10-week-old *neprilysin* $^{+/+}$ mice under the same conditions as for *A*. The amount of amyloid precursor protein in all groups remained unchanged as analyzed by Western blotting (data not shown). Each column with a bar represents the mean ± SE of 6 or 7 mice. $^*p < 0.05$, significantly different from rAAV-NEP-injected group.

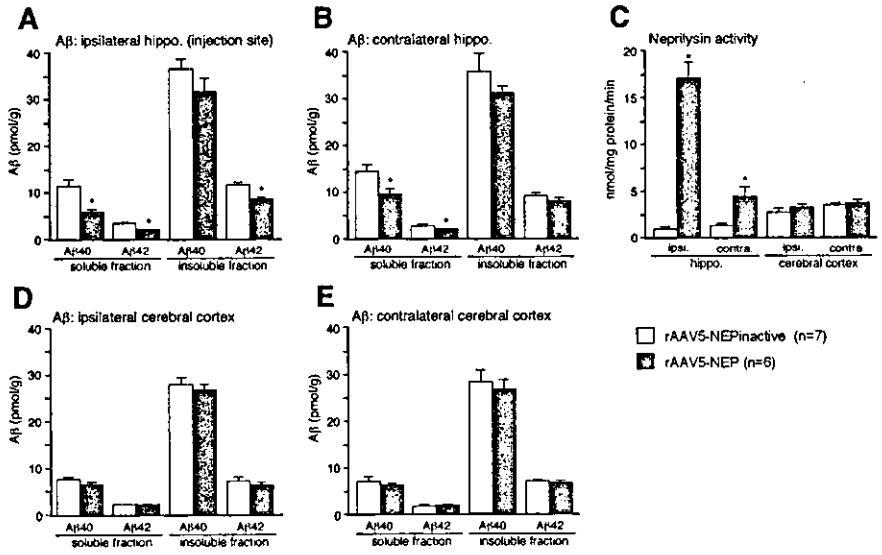

Figure 5. Changes in Aβ levels or endopeptidase activity in young Tg2576 mice after neprilysin gene transfer. Aβ levels in both soluble and insoluble fractions (*A*, *B*, *D*, *E*) and endopeptidase activities (*C*) of the ipsilateral (*A*) and contralateral (*B*) hippocampal formations, and the ipsilateral (*D*) and contralateral and (*E*) cerebral cortices were determined 8 weeks after unilateral injection of rAAV-NEPinactive (open column) and rAAV-NEP (shadowed column) (1.3×10^{10} genome copies) into the hippocampal formation of 10-week-old Tg2576 mice, respectively. Each column with a bar represents the mean ± SE of 6 or 7 mice. $^*p < 0.05$, significantly different from rAAV-NEPinactive-injected group.

to be transported (Fig. 5*D*,*E*). These findings indicate that neprilysin degrades soluble forms of Aβ with high efficiency.

Deceleration of Aβ deposition in aged mutant APP transgenic mouse brain

We examined whether neprilysin gene transfer decelerated amyloid deposition in aged Tg2576 mouse brain. Brain sections were immunostained with anti-Aβ antibody 12 weeks after unilateral viral injection into the hippocampal formation of 18-month-old Tg2576 mice. The Aβ deposition in the ipsilateral hippocampal formation, especially the stratum radiata, was remarkably decreased by neprilysin expressed after injection of rAAV-NEP, compared with that after injection of rAAV-NEPinactive (Fig. 6*A*,*B*). Quantitative assessment revealed that Aβ deposits in the entire hippocampal formation and the stratum radiata of the ipsilateral side after injection of rAAV-NEP were reduced by 25 and 49%, respectively, compared with those after rAAV-NEPinactive (Fig. 6*C*). Aβ loads in the cerebral cortices were similar in the rAAV-NEP and rAAV-NEPinactive-injected groups (Fig. 6*C*).

We further immunostained brain sections from Tg2576 mice that had received neprilysin gene transfer to analyze the spatial association of neprilysin with Aβ plaques (Fig. 7*A–E*). Robust synaptic components displaying immunoreactivity with anti-SNAP-25 antibody were detected around amyloid plaques, and neprilysin-positive immunoreactivity corresponded well with the SNAP-25-positive components. Neprilysin and SNAP-25 immunoreactivity frequently overlapped with Aβ immunoreactivity inside Aβ plaques, as shown by triple labeling. Such colocalization was seen in many amyloid plaques. Thus, immunoreactive neprilysin was presynaptic or derived from presynaptic components. On the other hand, we detected GFAP–positive astrocytes surrounding Aβ plaques, but they did not colocalize with neprilysin or GFAP (data not shown).

Discussion

Neprilysin is supposed to be involved in the catabolism of various neuropeptides, such as enkephalin, substance P, somatostatin, and kinins (Turner, 1998), and is currently regarded as a major Aβ-degrading enzyme (Iwata et al., 2000, 2001; Takaki et al., 2000; Shirotani et al., 2001; Carson and Turner, 2002; Saido, 2003; Saido and Nakahara, 2003; Saito et al., 2003). In the present study, we expressed neprilysin in the hippocampal formation of mice using rAAV-based vectors and successfully reduced Aβ levels in that region; neprilysin gene transfer abolished the increase in Aβ levels in neprilysin-deficient mice, reduced Aβ in young mutant APP transgenic mice and was also effective in the deceleration of Aβ deposition in the brain of aged mutant APP transgenic mice. Recently, in addition to neprilysin, several peptidases, such as endothelin-converting enzymes (ECEs) 1, 2, and insulin-degrading enzyme (IDE), have been identified as Aβ-degrading enzymes by reverse genetics studies (Eckman et al., 2003; Farris et al., 2003; Miller et al., 2003). Although these peptidases are likely to contribute to overall Aβ clearance in brain by complementing each other in a subcellular, cell type-

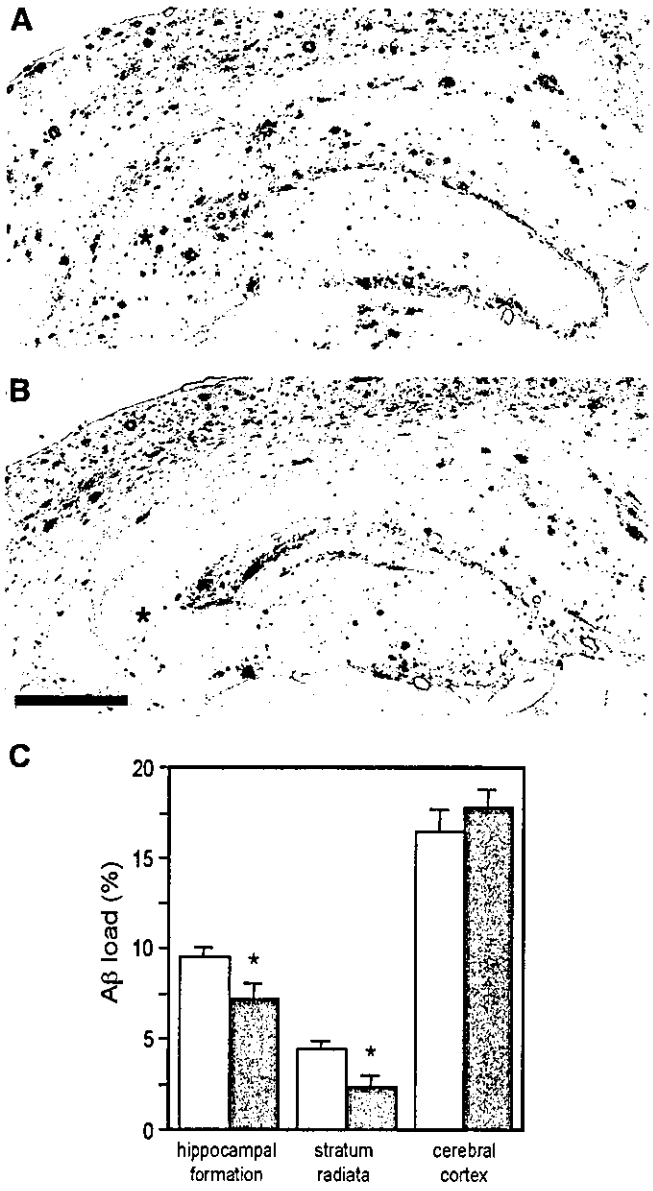

Figure 6. Deceleration of Aβ deposition in aged Tg2576 brains by neprilysin gene transfer. Twelve weeks after unilateral injection of rAAV-NEPinactive (*A*) or rAAV-NEP (*B*) (1.3×10^{10} genome copies) into the hippocampal formation of 18-month-old Tg2576 mice, brain sections were immunostained with anti-Aβ antibody, which recognized the C-terminal of Aβ42. Asterisks, stratum radiata. Scale bar, 500 μm. *C*, Aβ deposits in various areas of sections from the rAAV-NEPinactive-injected (shadowed column, $n = 7$) or rAAV-NEP-injected (open column, $n = 5$) brains were quantitated as described in Materials and Methods. Each column with a bar represents the mean ± SE. $^*p < 0.05$, significantly different from rAAV-NEPinactive-injected group.

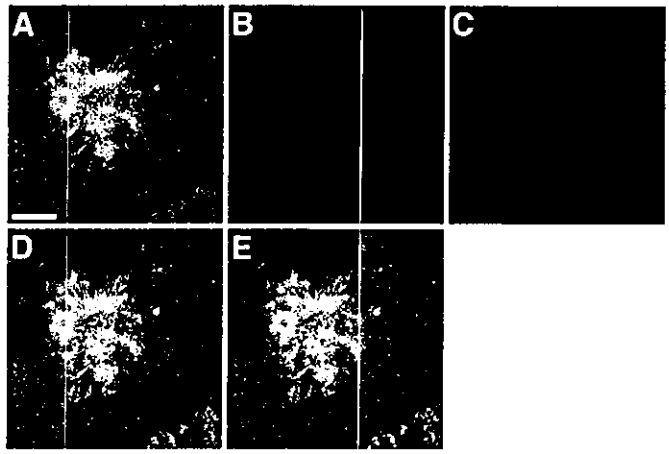

Figure 7. Detection of immunoreactive neprilysin from neuritic components surrounding amyloid plaques. Sections from rAAV-NEPinactive-injected brains of Tg2576 mice were immunolabeled with anti-SNAP-25 (*A*; green), anti-neprilysin (*B*; red), and anti-Aβ antibodies (*C*; blue). *D*, Merged images of sections labeled with anti-SNAP-25 and anti-neprilysin antibodies. *E*, Merged images of triply labeled section. Experimental conditions are the same as in the case of Figure 6. Scale bar, 20 μm.

and/or brain region-specific manner, the brain Aβ-elevating effect of neprilysin deficiency is greater than that of a deficiency of any other known Aβ-degrading enzyme (Iwata et al., 2001; Eckman et al., 2003; Farris et al., 2003; Miller et al., 2003; Saido and Nakahara, 2003; Saito et al., 2003). Neprilysin, a membrane-bound zinc metallopeptidase with its active site at the lumen side (Turner, 1998; Carson and Turner, 2002; Saido and Nakahara, 2003), is implicated in degradation of both intracellular and extracellular (membrane-associated) Aβ (Hama et al., 2001). The neprilysin-dependent degradation of exogenously administered synthetic $A\beta_{1-42}$ peptide *in vivo* (Iwata et al., 2000) demonstrates that neprilysin plays a larger role in the degradation of Aβ after secretion. In addition, because neprilysin was observed at the presynapses and on/around axons by double immunostaining with presynaptic markers (Fukami et al., 2002) or by subcellular fractionation and electron microscopic immunocytochemistry in brain (Barnes et al., 1988, 1992), it may play a key role in Aβ catabolism at and around neuronal synapses. The present report provides direct evidence for this.

In an earlier study of neprilysin gene transfer using a lentiviral vector, neprilysin expressed in the infected neurons was detected in cell bodies in most cases, as shown by immunostaining of the hippocampal formation (Marr et al., 2003). This is quite different from the results obtained with our vector; we found that that neprilysin was localized at the presynaptic sites, but not in the cell bodies. Therefore, Marr et al. (2003) probably observed mainly the intracellular degradation process of Aβ by neprilysin. Application of the rAAV vector-mediated gene transfer system, however, enabled us to evaluate catabolism of synaptic cleft-associated, presynaptic membrane-associated, and intravesicular Aβ by neprilysin around synaptic sites. Furthermore, in contrast to the study using the lentiviral vector, our gene transfer system produced remarkable effects on Aβ degradation not only on the injection side, but also in the contralateral hippocampus, suggesting that the rAAV-NEP vector offers substantial advantages for extensive reduction of Aβ levels. It is noteworthy that the relatively small increase of neprilysin activity in the contralateral hippocampal formation was sufficient to yield a significant reduction of Aβ. Our approach seems to enable widespread and efficient promotion of Aβ degradation, because exogenous neprilysin was axonally transported from the ipsilateral to the contralateral hippocampal formation and also to the intrahippocampal formation via appropriate neuronal circuits. Such axonal transport also occurs to the lateral entorhinal cortex-outer molecular layer of the dentate gyrus projection via the perforant path. Analysis of the hippocampal formation contralateral to the injection side in mutant APP transgenic mice in our work supported a possible role of neprilysin in Aβ degradation at the presynaptic sites, whereas Marr et al. (2003) examined the effects of neprilysin gene transfer on amyloid deposition in the ipsilateral hippocampal formation relative to the contralateral side, based on Aβ immunostaining. APP also undergoes axonal transport to

presynaptic terminals (Buxbaum et al., 1998), during which Aβ is generated through sequential cleavage by β- and γ-secretases (Hardy and Selkoe, 2002). Aβ released from presynaptic sites contributes to extracellular amyloid deposits, as demonstrated by *in vivo* experiments (Lazarov et al., 2002; Sheng et al., 2002). This process provides a rationale for the effective Aβ reduction by axonally transported rAAV-derived neprilysin. Although earlier studies found that dystrophic neurites in senile plaques were immunostained positively for neprilysin in AD brains and in brain of another strain of mutant APP-transgenic mouse (Akiyama et al., 2001; Fukami et al., 2002), neprilysin gene transfer more clearly visualized dystrophic neurites and amyloid plaques containing immunoreactive neprilysin. Thus, the sites for release and degradation of Aβ seem to be closely related to each other, and synaptic localization of neprilysin would be of particular importance for a connection with AD pathology.

We found that neprilysin gene transfer reduced both soluble and insoluble Aβ to similar extents in wild-type and neprilysin-deficient mouse hippocampal formations, whereas it reduced soluble Aβ more effectively than insoluble Aβ in the case of either the ipsilateral or the contralateral side of mutant APP transgenic mice. These results indicate that neprilysin preferentially attacks soluble Aβ, when Aβ is present at higher levels. Recent evidence suggests that soluble forms of Aβ are highly neurotoxic (Kuo et al., 1996; Lambert et al., 1998; Walsh et al., 1999; Hartley et al., 1999; Walsh et al., 2002), and may be more directly responsible for the pathological changes of AD, such as synaptic dysfunction and subsequent neuronal death (Kuo et al., 1996). The soluble forms of Aβ are composed of monomeric, oligomeric, and protofibrillar forms. Because neprilysin only degrades peptides smaller than 5 kDa, based on the size of its catalytic cavity (~20 Å) (Turner, 1998; Oefner et al., 2000), it is believed to degrade monomeric Aβ. However, there is a dynamic equilibrium between monomeric and oligomeric Aβ and further between oligomeric and protofibrillar Aβ (Walsh et al., 1999), and the deceleration of Aβ deposition by neprilysin gene transfer in aged mutant APP transgenic mice suggests that extensive removal of monomeric Aβ may reduce the levels of all of the soluble forms, and even insoluble forms, depending on the duration of the infection.

Synaptic dysfunction is indeed a typical and early function-related event in the AD cascade (Terry et al., 1991; Sze et al., 1997; Selkoe, 2002; Hardy and Selkoe, 2002), and is associated with a locally enhanced concentration of Aβ at the presynaptic terminals and inside synaptic vesicles in the AD brain. An increase in soluble Aβ levels rather than Aβ plaque load appears to cause such synaptotoxicity. Levels of soluble Aβ rather than insoluble Aβ are well correlated with synaptic changes and neuronal loss in AD brains (Lue et al., 1999; McLean et al., 1999). In several lines of mutant APP transgenic mice, structural changes in presynaptic terminals or neuronal loss are correlated with an increase in Aβ concentration in the brain, but not with plaque load (Hsia et al., 1999; Mucke et al., 2000; Buttini et al., 2002). Recent studies have indicated that particular forms of soluble Aβ, such as oligomeric or protofibrillar forms, cause dysfunction or modification of synaptic transmission and/or long-term potentiation *in vivo* (Walsh et al., 2002; Wang et al., 2002). The presence of neprilysin at the presynaptic sites would contribute to removal of a toxic form of Aβ through degrading monomeric Aβ, like clearance of neurotransmitters, in the extracellular space close to synapses, thereby eventually decelerating AD pathology.

The present data also suggest the presence of Aβ, either in particular compartments or of specific forms, which neprilysin cannot attack. In fact, the degree of Aβ removal in wild-type mice by neprilysin gene transfer was relatively low compared with that in neprilysin-deficient mice, and the degree of soluble Aβ removal by neprilysin gene transfer was similar in the ipsilateral and contralateral hippocampal formations of young APP transgenic mice, although the increases in neprilysin activity differed by [~10-fold. Because ECEs are supposed to degrade predominantly intracellular Aβ, which is present on the lumen side of a secreting vesicle, based on the acidic pH optima (Carson and Turner, 2002; Eckman et al., 2003; Saido and Nakahara, 2003), ECEs, as well as IDE, may be involved in degradation of Aβ in particular compartments, in which neprilysin does not play a major role.

In conclusion, we have demonstrated that presynaptic neprilysin efficiently and extensively degrades Aβ and decelerates Aβ deposition *in vivo*. These results indicate that upregulation of neprilysin activity at sites where a reduction in the neprilysin level may be caused by aging, might protect the synaptic function of AD-vulnerable neuronal circuits from Aβ pathology via a reduction of Aβ levels. We suggest that upregulation of neprilysin activity is a promising strategy for therapy and prevention of AD.

References

Akiyama H, Kondo H, Ikeda K, Kato M, McGeer PL (2001) Immunohistochemical localization of neprilysin in the human cerebral cortex: inverse association with vulnerability to amyloid β-protein (Aβ) deposition. Brain Res 902:277–281.

Amaral DG, Witter MP (1995) Hippocampal formation. In: The rat nervous system (Paxinos G, ed), pp 443–493. San Diego: Academic.

Barnes K, Turner AJ, Kenny AJ (1988) Electronmicroscopic immunocytochemistry of pig brain shows that endopeptidase-24.11 is localized in neuronal membranes. Neurosci Lett 94:64–69.

Barnes K, Turner AJ, Kenny AJ (1992) Membrane localization of endopeptidase-24.11 and peptidyl dipeptidase A (angiotensin converting enzyme) in the pig brain: a study using subcellular fractionation and electron microscopic immunocytochemistry. J Neurochem 58:2088–2096.

Buttini M, Yu GQ, Shockley K, Huang Y, Jones B, Masliah E, Mallory M, Yeo T, Longo FM, Mucke L (2002) Modulation of Alzheimer-like synaptic and cholinergic deficits in transgenic mice by human apolipoprotein E depends on isoform, aging, and overexpression of amyloid β peptides but not on plaque formation. J Neurosci 22:10539–10548.

Buxbaum JD, Thinakaran G, Koliatsos V, O'Callahan J, Slunt HH, Price DL, Sisodia SS (1998) Alzheimer amyloid protein precursor in the rat hippocampus: transport and processing through the perforant path. J Neurosci 18:9629–9637.

Carson JA, Turner AJ (2002) β-Amyloid catabolism: roles for neprilysin (NEP) and other metallopeptidases? J Neurochem 81:1–8.

Chiorini JA, Kim F, Yang L, Kotin RM (1999) Cloning and characterization of adeno-associated virus type 5. J Virol 73:1309–1319.

Eckman EA, Watson M, Marlow L, Sambamurti K, Eckman CB (2003) Alzheimer's disease β-amyloid peptide is increased in mice deficient in endothelin-converting enzyme. J Biol Chem 278:2081–2084.

Farris W, Mansourian S, Chang Y, Lindsley L, Eckman EA, Frosch MP, Eckman CB, Tanzi RE, Selkoe DJ, Guenette S (2003) Insulin-degrading enzyme regulates the levels of insulin, amyloid β-protein, and the β-amyloid precursor protein intracellular domain in vivo. Proc Natl Acad Sci USA 100:4162–4167.

Fukami S, Watanabe K, Iwata N, Haraoka J, Lu B, Gerard NP, Gerard C, Fraser P, Westaway D, St. George-Hyslop P, Saido TC (2002) Aβ-degrading endopeptidase, neprilysin, in mouse brain: synaptic and axonal localization inversely correlating with Aβ pathology. Neurosci Res 43:39–56.

Gomez-Isla T, Price JL, McKeel Jr DW, Morris JC, Growdon JH, Hyman BT (1996) Profound loss of layer II entorhinal cortex neurons occurs in very mild Alzheimer's disease. J Neurosci 16:4491–4500.

Hama E, Shirotani K, Masumoto H, Sekine-Aizawa Y, Aizawa H, Saido TC (2001) Clearance of extracellular and cell-associated amyloid β peptide through viral expression of neprilysin in primary neurons. J Biochem (Tokyo) 130:721–726.

Hardy J, Selkoe DJ (2002) The amyloid hypothesis of Alzheimer's disease: progress and problems on the road to therapeutics. Science 297:353–356.

Hartley DM, Walsh DM, Ye CP, Diehl T, Vasquez S, Vassilev PM, Teplow DB, Selkoe DJ (1999) Protofibrillar intermediates of amyloid β-protein induce acute electrophysiological changes and progressive neurotoxicity in cortical neurons. J Neurosci 19:8876–8884.

Hsia AY, Masliah E, McConlogue L, Yu GQ, Tatsuno G, Hu K, Kholodenko D, Malenka RC, Nicoll RA, Mucke L (1999) Plaque-independent disruption of neural circuits in Alzheimer's disease mouse models. Proc Natl Acad Sci USA 96:3228–3233.

Hsiao K, Chapman P, Nilsen S, Eckman C, Harigaya Y, Younkin S, Yang F, Cole G (1996) Correlative memory deficits, Aβ elevation, and amyloid plaques in transgenic mice. Science 274:99–102.

Iwata N, Tsubuki S, Takaki Y, Watanabe K, Sekiguchi M, Hosoki E, Kawashima-Morishima M, Lee H-J, Hama E, Sekine-Aizawa Y, Saido TC (2000) Identification of the major $A\beta_{1-42}$-degrading catabolic pathway in brain parenchyma: suppression leads to biochemical and pathological deposition. Nat Med 6:143–150.

Iwata N, Tsubuki S, Takaki Y, Shirotani K, Lu B, Gerard NP, Gerard C, Hama E, Lee H-J, Saido TC (2001) Metabolic regulation of brain Aβ by neprilysin. Science 292:1550–1552.

Iwata N, Takaki Y, Fukami S, Tsubuki S, Saido TC (2002) Region-specific reduction of Aβ-degrading endopeptidase, neprilysin, in mouse hippocampus upon aging. J Neurosci Res 70:493–500.

Kuo YM, Emmerling MR, Vigo-Pelfrey C, Kasunic TC, Kirkpatrick JB, Murdoch GH, Ball MJ, Roher AE (1996) Water-soluble Aβ (N-40, N-42) oligomers in normal and Alzheimer disease brains. J Biol Chem 271:4077–4081.

Lambert MP, Barlow AK, Chromy BA, Edwards C, Freed R, Liosatos M, Morgan TE, Rozovsky I, Trommer B, Viola KL, Wals P, Zhang C, Finch CE, Krafft GA, Klein WL (1998) Diffusible, nonfibrillar ligands derived from $A\beta_{1-42}$ are potent central nervous system neurotoxins. Proc Natl Acad Sci USA 95:6448–6453.

Lazarov O, Lee M, Peterson DA, Sisodia SS (2002) Evidence that synaptically released β-amyloid accumulates as extracellular deposits in the hippocampus of transgenic mice. J Neurosci 22:9785–9793.

Lu B, Gerard NP, Kolakowski Jr LF, Bozza M, Zurakowski D, Finco O, Carroll MC, Gerard C (1995) Neutral endopeptidase modulation of septic shock. J Exp Med 181:2271–2275.

Lue LF, Kuo YM, Roher AE, Brachova L, Shen Y, Sue L, Beach T, Kurth JH, Rydel RE, Rogers J (1999) Soluble amyloid β peptide concentration as a predictor of synaptic change in Alzheimer's disease. Am J Pathol 155:853–862.

Marr RA, Rockenstein E, Mukherjee A, Kindy MS, Hersh LB, Gage FH, Verma IM, Masliah E (2003) Neprilysin gene transfer reduces human amyloid pathology in transgenic mice. J Neurosci 23:1992–1996.

McLean CA, Cherny RA, Fraser FW, Fuller SJ, Smith MJ, Beyreuther K, Bush AI, Masters CL (1999) Soluble pool of Aβ amyloid as a determinant of severity of neurodegeneration in Alzheimer's disease. Ann Neurol 46:860–866.

Miller BC, Eckman EA, Sambamurti K, Dobbs N, Chow KM, Eckman CB, Hersh LB, Thiele DL (2003) Amyloid-β peptide levels in brain are inversely correlated with insulysin activity levels *in vivo*. Proc Natl Acad Sci USA 100:6221–6226.

Mucke L, Masliah E, Yu GQ, Mallory M, Rockenstein EM, Tatsuno G, Hu K, Kholodenko D, Johnson-Wood K, McConlogue L (2000) High-level neuronal expression of $A\beta_{1-42}$ in wild-type human amyloid protein precursor transgenic mice: synaptotoxicity without plaque formation. J Neurosci 20:4050–4058.

Oefner C, D'Arcy A, Hennig M, Winkler FK, Dale GE (2000) Structure of human neutral endopeptidase (Neprilysin) complexed with phosphoramidon. J Mol Biol 296:341–349.

Okada T, Nomoto T, Shimazaki K, Lijun W, Lu Y, Matsushita T, Mizukami H, Urabe M, Hanazono Y, Kume A, Muramatsu S, Nakano I, Ozawa K (2002) Adeno-associated virus vectors for gene transfer to the brain. Methods 28:237–247.

Saido TC (2003) Overview-Aβ metabolism: from Alzheimer research to brain aging control. In: Aβ metabolism and Alzheimer's disease (Saido TC, ed), pp 1–16. Texas: Landes Bioscience.

Saido TC, Nakahara H (2003) Proteolytic degradation of Aβ by neprilysin and other peptidases. In: Aβ metabolism and Alzheimer's disease (Saido TC, ed), pp 61–80. Texas: Landes Bioscience.

Saido TC, Iwatsubo T, Mann DM, Shimada H, Ihara Y, Kawashima S (1995) Dominant and differential deposition of distinct β-amyloid peptide species, $A\beta_{N3(pE)}$, in senile plaques. Neuron 14:457–466.

Saito T, Takaki Y, Iwata N, Trojanowski J, Saido TC (2003) Alzheimer's disease, neuropeptides, neuropeptidase, and amyloid-β peptide metabolism. Sci Aging Knowl Environ 2003 3:PE1.

Selkoe DJ (2002) Alzheimer's disease is a synaptic failure. Science 298:789–791.

Sheng JG, Price DL, Koliatsos VE (2002) Disruption of corticocortical connections ameliorates amyloid burden in terminal fields in a transgenic model of Aβ amyloidosis. J Neurosci 22:9794–9799.

Shirotani K, Tsubuki S, Iwata N, Takaki Y, Harigaya W, Maruyama K, Kiryu-Seo S, Kiyama H, Iwata H, Tomita T, Iwatsubo T, Saido TC (2001) Neprilysin degrades both amyloid β peptides 1–40 and 1–42 most rapidly and efficiently among thiorphan- and phosphoramidon-sensitive endopeptidases. J Biol Chem 276:21895–21901.

Sze CI, Troncoso JC, Kawas C, Mouton P, Price DL, Martin LJ (1997) Loss of the presynaptic vesicle protein synaptophysin in hippocampus correlates with cognitive decline in Alzheimer disease. J Neuropathol Exp Neurol 56:933–944.

Takaki Y, Iwata N, Tsubuki S, Taniguchi S, Toyoshima S, Lu B, Gerard NP, Gerard C, Lee H-J, Shirotani K, Saido TC (2000) Biochemical identification of the neutral endopeptidase family member responsible for the catabolism of amyloid β peptide in the brain. J Biochem (Tokyo) 128:897–902.

Terry RD, Masliah E, Salmon DP, Butters N, DeTeresa R, Hill R, Hansen LA, Katzman R (1991) Physical basis of cognitive alterations in Alzheimer's disease: synapse loss is the major correlate of cognitive impairment. Ann Neurol 30:572–580.

Turner AJ (1998) Neprilysin. In: Proteolytic enzymes (Barrett AJ, Rawlings ND, Woessner JF, eds), pp 1080–1085. London: Academic.

Walsh DM, Hartley DM, Kusumoto Y, Fezoui Y, Condron MM, Lomakin A, Benedek GB, Selkoe DJ, Teplow DB (1999) Amyloid β-protein fibrillogenesis. Structure and biological activity of protofibrillar intermediates. J Biol Chem 274:25945–25952.

Walsh DM, Klyubin I, Fadeeva JV, Cullen WK, Anwyl R, Wolfe MS, Rowan MJ, Selkoe DJ (2002) Naturally secreted oligomers of amyloid β protein potently inhibit hippocampal long-term potentiation in vivo. Nature 416:535–539.

Wang HW, Pasternak JF, Kuo H, Ristic H, Lambert MP, Chromy B, Viola KL, Klein WL, Stine WB, Krafft GA, Trommer BL (2002) Soluble oligomers of β amyloid (1–42) inhibit long-term potentiation but not long-term depression in rat dentate gyrus. Brain Res 924:133–140.

Weninger SC, Yankner BA (2001) Inflammation and Alzheimer disease: the good, the bad, and the ugly. Nat Med 7:527–528.

Yasojima K, Akiyama H, McGeer EG, McGeer PL (2001a) Reduced neprilysin in high plaque areas of Alzheimer brain: a possible relationship to deficient degradation of β-amyloid peptide. Neurosci Lett 297:97–100.

Yasojima K McGeer EG, McGeer PL (2001b) Relationship between β amyloid peptide generating molecules and neprilysin in Alzheimer disease and normal brain. Brain Res 919:115–121.

Available online at www.sciencedirect.com
SCIENCE DIRECT®
Biochemical and Biophysical Research Communications 315 (2004) 389–396
BBRC
www.elsevier.com/locate/ybbrc

Ras/MEK pathway is required for NGF-induced expression of tyrosine hydroxylase gene☆

Takahiro Suzuki,[a,*] Hiroki Kurahashi,[b] and Hiroshi Ichinose[a]

[a] *Department of Life Science, Graduate School of Bioscience and Biotechnology, Tokyo Institute of Technology, Yokohama, Japan*
[b] *Division of Molecular Genetics, Institute for Comprehensive Medical Science, Fujita Health University, Toyoake, Aichi 470-1192, Japan*

Received 16 January 2004

Abstract

Neurotrophins are essential for the development and survival of catecholaminergic neurons. However, the critical pathway for expression of the tyrosine hydroxylase (TH) gene induced by neurotrophin is still unclear. Here we found that Ras/MEK pathway is required for NGF-induced expression of the TH gene in PC12D cells. Induction of TH mRNA by NGF was abolished by pretreatment of the cells with U0126, an inhibitor for MEK1/2, but not with inhibitors for p38 MAPK, PI3K, and PKA. U0126 inhibited TH promoter activity at the same concentration as it acted on ERK1/2 phosphorylation. A dominant-negative form of Ras suppressed the NGF-induced activation of the TH reporter gene, and transient transfection of cells with wild-type Ras and an active form of MEK1 increased the TH promoter activity. The reporter assay also demonstrated that the Ras/MEK pathway acted on both the AP-1-binding motif and the cAMP-responsive element in the TH promoter.

Keywords: Catecholamine; Gene expression; MEK; Nerve growth factor; PC12 Cells; Ras; Tyrosine hydroxylase; Transcription

The gene expression of catecholamine-synthesizing enzymes is important for the determination of the expression of neurotransmitters during brain development as well as for brain function under physiological and pathological conditions. Tyrosine hydroxylase (TH) is the rate-limiting enzyme for catecholamine biosynthesis, and the transcriptional regulation of the TH gene is one of the important molecular events for the determination of the catecholaminergic phenotype at the embryonic stage and the TH enzyme expression level in catecholaminergic cells at postnatal developmental and adult stages. An important goal in the study of this gene is the elucidation of the signaling cascades involved in TH gene transcription.

Various stimuli, such as cAMP-elevating reagents and hormones, neurotrophic factors, glucocorticoids, retinoic acid, and synaptic activity, have been shown to increase the TH gene expression in cultured cells and tissues [1]. The cyclic AMP/protein kinase A (PKA) signaling pathway is a well-studied cascade that leads to transcription of the TH gene. Derivatives of cAMP and cAMP-elevating reagents such as forskolin (FSK) enhance the TH expression in cultured cells including PC12 and neural stem cells [2–7]. A cyclic AMP-responsive element (CRE) located at position −45/−38 in the TH promoter mediates basal and cAMP-induced TH transcription [2–5]. CREB was identified as a transcription factor that mediates the basal and cAMP-induced TH transcription via the TH-CRE [8–11].

Neurotrophins have been shown to regulate neurite outgrowth, survival, and plasticity of various neural cells [12]. Nerve growth factor (NGF) is the prototype of the neurotrophin family and binds to 2 classes of transmembrane receptors, TrkA and p75, a receptor tyrosine kinase and a member of TNF receptor family, respectively [13]. Studies using gene-targeted mutant mice demonstrated that NGF and TrkA were required

☆ *Abbreviations:* TH, tyrosine hydroxylase; NGF, nerve growth factor; MAPK, mitogen activated protein kinase; ERK, extracellular signal regulated kinase; MEK, MAP and ERK kinase; PI3K, phosphatidylinositol 3-kinase; CRE, cAMP-responsive element; CREB, CRE-binding protein; AP1, AP-1-binding site; PKA, protein kinase A; kb, kilobase(s); bp, base pair(s); FSK, forskolin.

* Corresponding author. Fax: +81-45-924-5807.
E-mail address: tsuzuki@bio.titech.ac.jp (T. Suzuki).

0006-291X/$ - see front matter © 2004 Elsevier Inc. All rights reserved.
doi:10.1016/j.bbrc.2004.01.068

for the development and survival of peripheral sympathetic neurons at late embryonic and postnatal stages [14–18]. The PC12 cell line is a neural crest-derived adrenal chromaffin cell line that was obtained from a rat pheochromocytoma and is a useful model to study the molecular mechanisms responsible for sympathetic neuronal differentiation induced by NGF. NGF activates multiple intracellular signaling molecules in PC12 cells [13]; and Ras/MEK and PI3K/Akt pathways are well-studied cascades regulating neurite outgrowth, cell survival, and neuronal gene expression in response to NGF [12,13]. Both Ras/MEK and PI3K/Akt pathways were suggested to up-regulate the gene expression of NMDA receptor 1 and acetylcholine receptors in response to NGF in PC12 cells [19,20].

There are a few reports on the NGF-mediated transcription of the TH gene. NGF potentiated both the TH mRNA level and TH promoter activity in PC12 cells [21]. It was also reported that NGF-dependent activation of the TH promoter was blocked by a mutation of the AP-1-binding site (AP1) located at −205/−199 in its promoter [22]. However, the nature of the signaling cascade(s) for the TH gene expression induced by NGF is still unclear.

In the present study, we demonstrated that TH gene expression elevated by NGF was mediated by Ras/MEK pathway using PC12D, a subclone of the PC12 cell line [23]. Our data suggested that NGF-induced TH gene expression was not dependent on the PI3K/Akt pathway. We also demonstrated that the Ras/MEK pathway acted on both AP1 and CRE in the TH promoter in response to NGF. Our results suggest that the Ras/MEK pathway would have an important role in the TH gene expression in response to neurotrophins during neural development.

Materials and methods

Plasmids. Firefly luciferase reporter genes containing mouse TH promoter regions (mTHpro4.3-Luc, mTHpro0.8-Luc, and mTHpro0.8CREmt-Luc) were constructed as previously described [24]. A mutation in the AP-1-binding motif of mTHpro0.8-Luc (GAATTCA) was generated by a PCR method using a forward primer (TAGC CCGGGCTCGAGACCATGATGCAGG) and a mutated reverse primer (TTAGATCTAATTGCATCCACTGTCGCAGGCACCTGC CTCTGAATTCCCCTCCGCCCTAGACACG) and the wild-type vector, mTHpro4.3-Luc (TGATTCA). The mutation was verified by sequencing using an ABI PRISM 310 genetic analyzer (Applied Biosystems). To produce mTHpro0.8AP1mt-Luc and mTHpro0.8AP1mtCREmt-Luc, we inserted a fragment containing the AP1 mutation into mTHpro0.8-Luc and mTHpro0.8CREmt-Luc, respectively, between the *XhoI* and *BglII* sites. Firefly luciferase reporter plasmids containing the AP1 or CRE upstream of a TATA-like promoter (P_{TAL}) region taken from the herpes simplex thymidine kinase promoter were purchased from CLONTECH.

Cell culture and transfections. PC12D cells were cultured in DMEM containing 10% horse serum and 5% fetal bovine serum. A sea pansy luciferase vector, pRL-TK (Toyoink, Tokyo), was used as an internal control to normalize for variations in transfection efficiency. Cells were transfected by lipofection using LipofectAMINE 2000 (Gibco). One day prior to transfection, the cells were plated on 24-well plates and transfected at ~50% confluence. At 48 h after transfection, the cells were harvested and assayed for firefly and sea pansy luciferase activities by using a PicaGene Dual luciferase assay kit (Toyoink, Tokyo).

Quantitative real-time PCR analysis. Total RNA was isolated from cells by using Trizol reagent (Gibco). The total RNA was subjected to reverse transcription by using Superscript II (Gibco). Real-time PCR of TH transcripts and 18S ribosomal RNA as an internal control was performed on an ABI PRISM 7700 using a TaqMan Universal PCR Master Mix (Applied Biosystems). The reactions were performed in a total volume of 25 μl in the presence of 2 μl of diluted (1:100) reverse-transcribed product. In the reaction for TH transcripts, primers TCGGAAGCTGATTGCAGAGAT (forward) and TTCCGCTGTG TATTCCACATG (reverse) were added to a final concentration of 900 nM each, and a TaqMan probe 5′-(FAM)-CCTTCCAGTACA AGCACGGTGAACCAATT-(TAMRA)-3′ (ordered from Applied Biosystems) was added to a final concentration of 250 nM. For 18s ribosomal RNA, a Pre-Developed TaqMan Assay Reagent (Applied Biosystems) was used. The reactions were performed according to the manufacturer's instructions.

Western Blotting. For preparation of whole-cell extracts for immunoblot analysis of phosphorylated proteins, the cell pellet was directly lysed in SDS-sample buffer and the supernatant was collected as the whole-cell extract. Phosphorylated form-specific and nonspecific antibodies against ERK1/2 and Akt were purchased from Cell Signaling Technology. Immunoblotting was performed following the supplier's protocol. The cell lysate was separated by SDS–PAGE and transferred to a PVDF membrane (Bio-Rad). Proteins were visualized with ECL plus (Amersham Biosciences).

Statistics. Student's t test was used for statistical evaluations. A level of $p < 0.05$ was accepted as statistically significant.

Results

An inhibitor of MEK blocked induction of TH mRNA in response to NGF

First, we examined induction of TH mRNA by NGF in PC12D cells. Real-time PCR analysis demonstrated that induction of TH mRNA was detectable within 1 h after exposure to NGF. The level reached its maximum at 2–3 h and remained there for at least 24 h after the start of exposure (Fig. 1A). To explore the signaling cascades activated by NGF to regulate the TH gene expression, we examined the effect of inhibitors specific for protein kinases known to be activated in response to NGF. We found that the induction of TH mRNA caused by the addition of NGF was abolished by pretreatment with U0126, an inhibitor of MEK1/2, but not by that with SB203580, wortmannin, and H-89, which are inhibitors for p38 MAPK, PI3K, and PKA, respectively (Fig. 1B). By Western blot analysis using phosphorylated form-specific and nonspecific antibodies against ERK1/2, which are substrates for MEK1/2, we confirmed that phosphorylation and supershift of ERK1/2 that occurred by the treatment with NGF were abolished by the pretreatment with 10 μM U0126, whereas both were unchanged by the pretreatment with

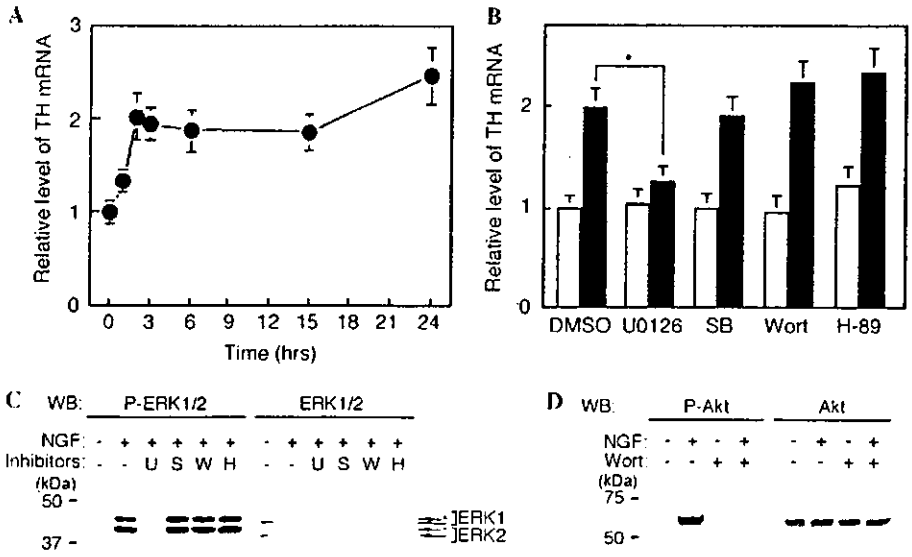

Fig. 1. Induction of TH mRNA in response to NGF attenuated by pretreatment with U0126 in PC12D cells. (A,B) Analyses by real-time quantitative PCR were performed as described in Materials and methods. (A) Time course analysis. Cells were incubated with 10 ng/ml rat recombinant NGF. Data are means ± SD values from 3 independent experiments. (B) TH mRNA levels in NGF-stimulated (closed bars) and non-stimulated control (open bars) PC12D cells in the presence of kinase inhibitors were measured. Levels of the TH mRNA are expressed as fold activation relative to that in non-stimulated PC12D cells in the vehicle only. 18S rRNA was used to the internal control for normalization. Cells were pretreated with 10 μM U0126, 10 μM SB203580 (SB), 0.1 μM wortmannin (Wort), or 30 μM H-89 for 30 min, and then incubated with 10 ng/ml NGF for 3 h. Data are means ± SD values from 4 independent experiments. Values of p were calculated based on the value for the NGF-stimulated cells in the vehicle only (DMSO): $^{*}p < 0.001$. (C,D) Western blotting was performed by using phosphorylated form-specific or nonspecific antibodies against ERK and Akt. Whole-cell extracts were prepared from PC12D cells that had been pretreated with the inhibitors or vehicle only for 30 min and then incubated without or with 10 ng/ml NGF for 15 min. Whole-cell extracts were separated by SDS–PAGE (10% gel) and then analyzed by immunoblotting with antibodies against phosphorylated and total ERK (C, left and right panels, respectively), and phosphorylated and total Akt (D, left and right panels, respectively). (C) Arrows with an asterisk indicate supershifted bands. Data are representative of those obtained from 3 additional independent experiments.

the other inhibitors (Fig. 1C). We also confirmed that wortmannin completely blocked phosphorylation of Akt induced by NGF (Fig. 1D).

Ras- and MEK-dependent activation of the TH promoter by NGF

We next examined the effects of the kinase inhibitors on the NGF-stimulated TH promoter activity. To examine the transcription of the TH gene in PC12D cells, we transfected the cells with plasmid constructs containing a 4.3-kb section of the mouse TH 5′-flanking region fused to a luciferase reporter gene (mTHpro4.3-Luc, Fig. 2A). For comparison, we also examined their effects on the induction of TH promoter activity by FSK, a potent cAMP-elevating reagent. As shown in Fig. 2A, reporter activity was greatly increased in response to NGF in PC12D cells. Pretreatment of PC12D cells with 10 μM U0126 greatly blocked the NGF-dependent activation of the TH promoter, whereas 30 μM H-89 only partially blocked it (Fig. 2B). We also demonstrated that SB203580 (10 μM) and wortmannin (0.1 μM) had no effect on the TH promoter activity in the presence or absence of NGF (data not shown). These data suggest that MEK activity was required for TH gene transcription in response to NGF. In contrast, FSK-dependent induction of the TH promoter activity was highly inhibited by the pretreatment with H-89, but only partially with U0126 (Fig. 2B), confirming the PKA-dependency of the cAMP-induced TH gene transcription. U0126 inhibited the TH promoter activity induced by NGF at the same concentration effective in inhibiting the ERK1/2 phosphorylation (Figs. 2C and D).

The blockage by U0126 suggested that the Ras/MEK pathway might be involved in the NGF-stimulated TH promoter activity. To test this possibility further, we examined the effects of Ras and MEK overexpression on the TH promoter activity. Co-transfection of the PC12D cells with wild-type and the dominant-negative form of Ras demonstrated that NGF-stimulated TH promoter activity was attenuated by the dominant negative, but not by the wild-type, form in a dose-dependent manner (Fig. 3A). In contrast, the wild-type, but not the dominant-negative, one itself activated the TH promoter activity in a dose-dependent manner (Fig. 3A). When the co-transfection was done with a dominant-negative form of Akt (50 ng of DNA) the NGF-induced activation of the TH reporter gene was not suppressed (Fig. 3B, the left panel). In addition, an active form of MEK1 (50 ng of DNA), as well as the wild-type Ras, increased the TH promoter activity by itself (Fig. 3B, the

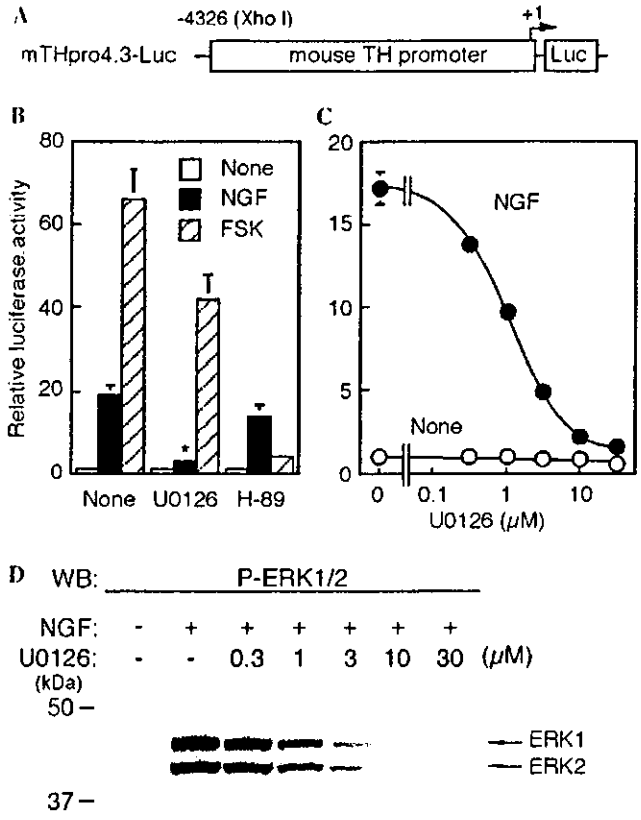

Fig. 2. Induction of TH promoter activity in response to NGF attenuated by pretreatment with U0126. (A) Diagram of a reporter plasmid containing 4.3 kb of the TH 5′-flanking region (mTHpro4.3-Luc). (B) Relative reporter activity of mTHpro4.3-Luc in NGF-stimulated (closed bars), FSK-stimulated (hatched bars), and non-stimulated control (open bars) PC12D cells was measured. A sea pansy luciferase vector, pRL-TK, was used as an internal control to normalize for variations in transfection efficiency. The cells were co-transfected with the luciferase reporter vector and the internal control vectors 24 h prior to pretreatment with 10 μM U0126 or 30 μM H-89 for 30 min and subsequent treatment with 10 ng/ml NGF or 10 μM FSK for 6 h. Data are means ± SD values from 3 independent experiments. Values of p were calculated with reference to the value for the vehicle-stimulated cells: $^{*}p < 0.01$. (C,D) Dose-dependent inhibition of the NGF-induced TH promoter activity and ERK phosphorylation, respectively, by U0126. Cells were pretreated with 0, 0.3, 1, 3, 10, or 30 μM U0126 for 30 min and then incubated with NGF. (C) The reporter-transfected cells were incubated with NGF for 6 h. Data are means ± SD values from 2 independent experiments, each with measurements done in triplicate. (D) Cells were incubated with NGF for 15 min and subjected to Western blotting analysis using anti-phosphorylated ERK1/2. Data are representative of those obtained in 2 additional independent experiments.

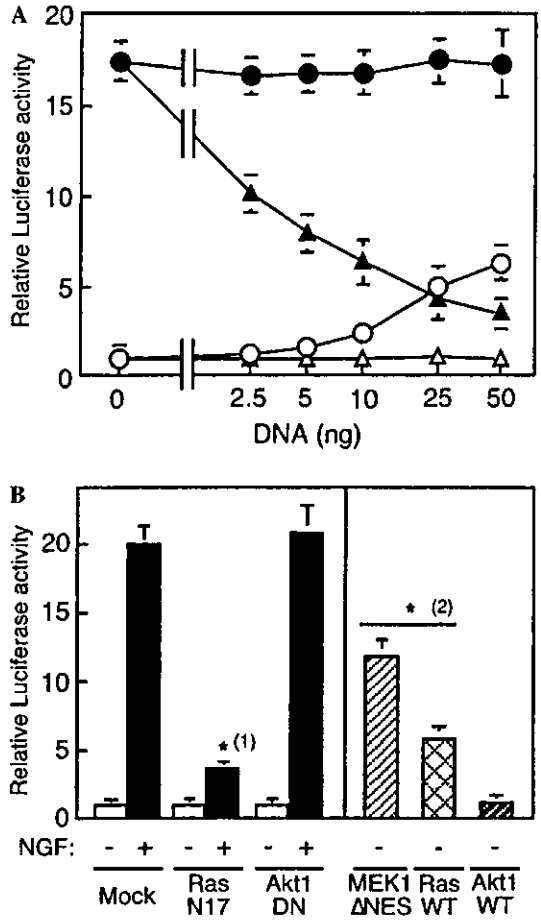

Fig. 3. Effects of Ras and MEK overexpression on the TH promoter activity. (A) The indicated DNA amounts of the wild-type and a dominant-negative Ras-expression vector, pCMV-Ras (circles) and pCMV-RasN17 (triangles), respectively, along with the mTHpro4.3-Luc reporter gene were used for co-transfection of PC12D cells. pRL-TK, an internal control vector to normalize for variations in transfection efficiency, was also included. An empty vector, pCMV-C, which has no Ras-cDNA sequence, was constructed and used as a carrier vector. Transfected cells were cultured for 48 h and then stimulated with NGF (closed symbols) or vehicle only (open symbols) for 6 h. Data are the means ± SD values from 2 independent experiments, in which measurements were done in triplicate. (B) PC12D cells were co-transfected with pRL-TK, the reporter gene, and 50 ng RasN17- or Akt kinase inactive-expression vector (RasN17 or AktDN, respectively), or control vector (pBluescript, Mock); and the cells were then incubated with or without NGF for 6 h (closed or open bars, respectively, in the left panel) and then harvested for the luciferase assay. Alternatively, the reporter vector was used for co-transfection with an active form of MEK1-, wild-type Ras-, or wild-type Akt-expression vector; and the transfected cells were then incubated without NGF (the right panel). Values of p were calculated based on the value of NGF-stimulated$^{(1)}$ and non-stimulated$^{(2)}$ PC12D cells transfected with the control vector: $^{*}p < 0.001$.

right panel). Co-transfection with the dominant-negative Ras did not attenuate the active MEK1-induced activation of the TH promoter (data not shown).

Both TH-AP1 and TH-CRE mediate transcriptional activation of the TH gene induced by NGF

We next evaluated the contribution of TH-AP1 and TH-CRE to the increased transcription of the TH gene mediated by Ras/MEK pathway in NGF-stimulated PC12D cells. We constructed wild-type, CRE and AP1 single-mutated, and CRE and AP1 double-mutated TH reporter vectors containing about 0.8 kb of the mouse TH 5′-flanking region upstream from the transcriptional start site (mTHpro0.8-Luc. Fig. 4A). Stimulation by NGF markedly increased the reporter activity of the

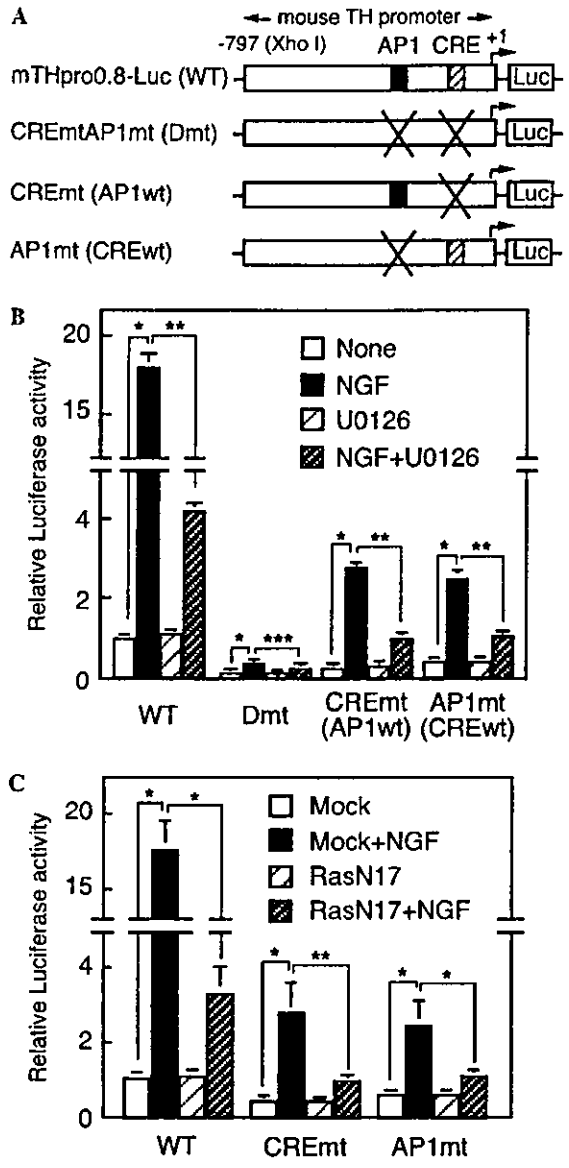

Fig. 4. Activities of CRE- and AP1-mutated reporter genes in the TH promoter region in response to NGF in PC12D cells. (A) Reporter plasmids containing 0.8 kb of the TH 5′-flanking region (mTHpro0.8-Luc) without or with a CRE and AP1 double mutation, or a mutation in the CRE consensus motif or AP1 site (WT, Dmt, CREmt, or AP1mt, respectively) were constructed. (B) Reporter activities of the wild-type and mutant TH promoter constructs were evaluated in NGF- and non-stimulated PC12D cells pretreated for not with U0126. Data are means ± SD values from 3 to 6 independent experiments. (C) PC12D cells were co-transfected with reporter genes containing the wild-type or mutant TH promoters and the RasN17-expression vector or pCMV-C control vector (Mock), and then cultured for 48 h and thereafter stimulated with NGF for 6 h. Data are means ± SD values from 3 independent experiments. Values of p are given as indicated by the brackets: values of p were calculated: $^{*}p < 0.001$, $^{**}p < 0.01$, and $^{***}p < 0.05$.

wild-type mTHpro0.8-Luc (Fig. 4B, the left panel); and the NGF-dependent activation was also greatly attenuated by the pretreatment with U0126, as had been the case for mTHpro4.3-Luc (Fig. 2A). The reporter activity of the double mutant was very low in non-stimulated cells and NGF-dependent activation was also very weak (Fig. 4B). This small activation was attenuated only slightly by U0126 (Fig. 4B). In contrast to the double mutant, the luciferase activity with single mutant constructs for TH-CRE or TH-AP1 remained highly activated by NGF; and the induction by NGF was blocked by the pretreatment with U0126, whereas the mutation in CRE or AP1 significantly attenuated the TH promoter activity without NGF stimulation (Fig. 4B). NGF-induced TH promoter activities of the CRE and AP1 single mutant constructs were similarly suppressed by co-transfection with the dominant-negative Ras (Fig. 4C), and transient transfection with the wild-type Ras and the active MEK1 increased the TH promoter activity without NGF-stimulation (data not shown). These data suggest that Ras/MEK pathway acted on the TH-AP1 and TH-CRE in response to NGF.

To test this possibility further, we measured promoter activities of reporter genes containing tandem repeats of AP1 and CRE consensus motives (Fig. 5A). We found that the transcriptional activities mediated by the consensus AP1 and CRE were induced by NGF and that both transcriptional activities were attenuated by the pretreatment with U0126 (Fig. 5B). We also demonstrated

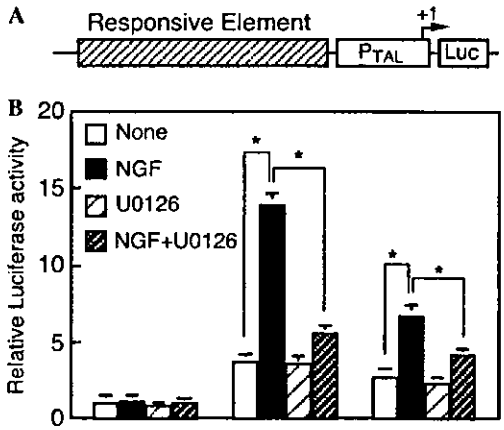

Fig. 5. Activation of AP1- and CRE-mediated transcription in response to NGF in a U0126-sensitive manner in PC12D cells. (A) Reporter vectors have a specific *cis*-acting element, CRE or AP1, upstream from the TATA-like promoter region taken from the herpes simplex virus thymidine kinase (P_{TAL}) and connected to firefly luciferase cDNA. The control vector lacks the responsive element and has P_{TAL} only. (B) The relative activity of the reporter genes in response to NGF with the pretreatment with U0126 or vehicle only was evaluated. The activity of the reporter genes was expressed as fold activation with respect to the activity of the control vector with no treatment. Transfection efficiency was normalized by using pRL-TK. Data are means ± SD values from 3 independent experiments. Values of p for activity induced by NGF were calculated based on the values for the non-stimulated control cells; and those for inhibition of the NGF response by the pretreatment with U0126 were calculated with reference to the values for the non-U0126-pretreated, NGF-treated cells: $^{*}p < 0.001$.

that the wild-type Ras and the active MEK overexpression increased the activity of the reporter constructs containing consensus AP1 and CRE (data not shown).

Discussion

In the present study, we demonstrated that the Ras/MEK pathway was required for the NGF-mediated transcriptional activation to express the TH gene in PC12D, a subclone of the PC12 cell line. We also showed that the Ras/MEK pathway acted on AP1 and CRE in the TH promoter to transcribe the TH gene in response to NGF.

NGF has been demonstrated to up-regulate the TH gene expression in peripheral sympathetic and sensory neurons. In addition, TrkB ligands, i.e., BDNF and NT-4/5, recently have been shown to increase the TH expression in developing noradrenergic neurons in the locus coeruleus [25]. Whereas molecular mechanisms and signaling pathways in response to neurotrophins to regulate neurite extension and neural cell survival by neurotrophins have been extensively investigated [12], those involved in the transcriptional expression of the TH gene are relatively little known. In the present study, we demonstrated, for the first time, that the Ras/MEK pathway is required for transcription of the TH gene in response to NGF. Since other neurotrophins and other neurotrophic factors such as GDNF are known to activate the MEK pathway and to regulate TH gene expression, our data suggest that the Ras/MEK pathway may play an important role in TH gene expression elicited by various stimuli including other neurotrophic factors.

Co-operative action of Ras/MEK and PI3K/Akt pathways was suggested to up-regulate the gene expression of NMDA receptor 1 and acetylcholine receptors in response to NGF in PC12 cells [19,20]. In contrast, our data suggest that NGF-induced TH gene expression is dependent on the Ras/MEK pathway, but not on the PI3K/Akt pathway, because the PI3K inhibitor wortmannin did not attenuate induction of TH mRNA (Fig. 1B), and also wortmannin and inactive Akt kinase had no effect on TH promoter activation by NGF (data not shown and Fig. 3B), whereas wortmannin completely blocked phosphorylation of Akt induced by NGF (Fig. 1D).

The Ras/MEK pathway is well known to be required for the expression of AP-1 transcription factors in PC12 cells treated with NGF. MEK inhibitors reduced AP-1 binding to a TH-AP1 oligonucleotide in response to acidic fibroblast growth factor in cultured striatal neurons [26], and overexpression of AP-1 transcription factors such as Fra-2 and c-Fos stimulated TH transcription in PC12 cells [27,28]. We demonstrated by promoter assay that TH-AP1 was required for induction of the TH promoter activity by NGF via Ras/MEK pathway (Fig. 4B) and by Western blotting analysis that the induction of c-Fos and c-Jun in response to NGF reached its maximum at 2–3 h after the start of exposure and was greatly attenuated by the pretreatment with U0126 in PC12D cells (data not shown). These data also suggested that AP-1 transcription factors would have an important role in the induction of TH gene transcription via the Ras/MEK pathway.

We demonstrated that TH-CRE as well as TH-AP1 was required for the induction of TH gene expression mediated by Ras/MEK pathway in response to NGF in PC12D cells (Fig. 4B). In contrast, the TH-CRE site was previously thought to be independent of or negatively regulated by NGF signaling, because mutation in the TH-CRE did not block the action of NGF in PC12 cells [22]. Additionally, cloned PC12 cells expressing a dominant-negative form of p90RSK, the wild-type of which is activated by the Ras/MEK pathway in response to NGF, showed hypersensitivity to FSK in the induction of TH mRNA [29]. We suppose that the co-operative action of TH-AP1 and TH-CRE to mediate transcription is necessary to efficiently transcribe the TH gene, because TH promoter activity induced by NGF in PC12D cells was much higher than those in PC12 cells (data not shown). We are now investigating the molecular mechanism for co-operative regulation of NGF-stimulated transcription by TH-AP1 and TH-CRE in PC12D cells.

NGF was shown to cause phosphorylation of CREB at least in part via the Ras/MEK-dependent pathway [30], and Ras/MEK/CREB pathway was required for the induction of c-Fos in response to NGF via the CRE site in the c-Fos promoter in PC12 cells [30,31]. CREB was also shown to be required for NGF-dependent survival of sympathetic neurons [32]. In addition, phosphorylation of ATF-2 on Thr69 could be done via a MEK-dependent pathway in PC12 cells [33], and we recently reported that activation of ATF-2 up-regulated the TH gene transcription via CRE, and suggested that ATF-2/TH-CRE-mediated transcription might have an important role in the TH gene expression during postnatal neural development [24]. We are now investigating the role of CREB and ATF-2 as candidate molecules for regulation of the TH-CRE-mediated transcription of the TH gene in response to NGF.

A study using transgenic mice carrying the LacZ gene driven by a TH promoter with mutations in either the CRE or AP1 sites demonstrated that the CRE- and AP1-mutated transgenes were not expressed in adult mice, but were expressed in embryos [34]. Mice carrying targeted mutations in the NGF gene showed a phenotype very similar to that mice with a mutated TrkA gene, the phenotype being a substantial reduction, by the first postnatal week, in the number of peripheral sympathetic neurons derived from the neural crest [16,17]. Based on

these studies, we suggest that the both TH-AP1- and TH-CRE-mediated transcription via the neurotrophin/Ras/MEK signaling cascade may be critical for the TH gene expression during postnatal development.

MAPK has been demonstrated to phosphorylate the TH protein and to elevate the catalytic activity of the enzyme, and the phosphorylation of TH was reported to occur within 15 min in response to phorbol esters or NGF [35]. Our data suggest that the Ras/MEK pathway up-regulates the TH activity at both transcriptional level as well as at post-transcriptional level.

Although the TH mRNA level was significantly elevated in PC12D cells by 3–24 h after the addition of NGF, the TH enzyme activity was unchanged (data not shown). Since the change in TH protein level and enzymatic activity was very small in mice carrying a TH transgene in spite of a great increase in TH mRNA level [36], some unknown additional mechanism may exist to up-regulate both the TH protein level and enzyme activity.

Acknowledgments

This work was supported by grants from the programs Grants-in-Aid for Encouragement of Young Scientists (to T.S.) and Grants-in-Aid for Scientific Research on Priority Areas (C)—Advanced Brain Science Project—(to H.I.) from the Ministry of Education, Culture, Sports, Science and Technology of Japan; Health Science Research Grants—Research on Human Genome, Tissue Engineering, Food Biotechnology—from the Ministry of Health, Labour and Welfare of Japan (to H.I.); and by the Human Frontier Science Program (to H.I.); Grants-in-Aid for Bio-venture Research Center of Fujita Health University from the Ministry of Education, Culture, Sports, Science and Technology of Japan and Fujita Health University.

References

[1] T. Nagatsu, Tyrosine hydroxylase: human isoforms, structure and regulation in physiology and pathology, Essays Biochem. 30 (1995) 15–35.

[2] K.S. Kim, M.K. Lee, J. Carroll, T.H. Joh, Both the basal and inducible transcription of the tyrosine hydroxylase gene are dependent upon a cAMP response element, J. Biol. Chem. 268 (1993) 15689–15695.

[3] K.S. Kim, D.H. Park, T.C. Wessel, B. Song, J.A. Wagner, T.H. Joh, A dual role for the cAMP-dependent protein kinase in tyrosine hydroxylase gene expression, Proc. Natl. Acad. Sci. USA 90 (1993) 3471–3475.

[4] S.E. Hyman, M. Comb, Y.S. Lin, J. Pearlberg, M.R. Green, H.M. Goodman, A common trans-acting factor is involved in transcriptional regulation of neurotransmitter genes by cyclic AMP, Mol. Cell. Biol. 8 (1988) 4225–4233.

[5] E.J. Lewis, C.A. Harrington, D.M. Chikaraishi, Transcriptional regulation of the tyrosine hydroxylase gene by glucocorticoid and cyclic AMP, Proc. Natl. Acad. Sci. USA 84 (1987) 3550–3554.

[6] K. Sakurada, M. Ohshima-Sakurada, T.D. Palmer, F.H. Gage, Nurr1, an orphan nuclear receptor, is a transcriptional activator of endogenous tyrosine hydroxylase in neural progenitor cells derived from the adult brain, Development 126 (1999) 4017–4026.

[7] L. Lo, X. Morin, J.F. Brunet, D.J. Anderson, Specification of neurotransmitter identity by Phox2 proteins in neural crest stem cells, Neuron 22 (1999) 693–705.

[8] D.J. Swanson, E. Zellmer, E.J. Lewis, The homeodomain protein Arix interacts synergistically with cyclic AMP to regulate expression of neurotransmitter biosynthetic genes, J. Biol. Chem. 272 (1997) 27382–27392.

[9] M. Lazaroff, S. Patankar, S.O. Yoon, D.M. Chikaraishi, The cyclic AMP response element directs tyrosine hydroxylase expression in catecholaminergic central and peripheral nervous system cell lines from transgenic mice, J. Biol. Chem. 270 (1995) 21579–21589.

[10] K. Nagamoto-Combs, K.M. Piech, J.A. Best, B. Sun, A.W. Tank, Tyrosine hydroxylase gene promoter activity is regulated by both cyclic AMP-responsive element and AP1 sites following calcium influx. Evidence for cyclic amp-responsive element binding protein-independent regulation, J. Biol. Chem. 272 (1997) 6051–6058.

[11] K.M. Piech-Dumas, A.W. Tank, CREB mediates the cAMP-responsiveness of the tyrosine hydroxylase gene: use of an antisense RNA strategy to produce CREB-deficient PC12 cell lines, Mol. Brain Res. 70 (1999) 219–230.

[12] M. Bibel, Y.A. Barde, Neurotrophins: key regulators of cell fate and cell shape in the vertebrate nervous system, Genes Dev. 14 (2000) 2919–2937.

[13] W.J. Friedman, L.A. Greene, Neurotrophin signaling via Trks and p75, Exp. Cell Res. 253 (1999) 131–142.

[14] T.D. Patel, A. Jackman, F.L. Rice, J. Kucera, W.D. Snider, Development of sensory neurons in the absence of NGF/TrkA signaling in vivo, Neuron 25 (2000) 345–357.

[15] W.D. Snider, Functions of the neurotrophins during nervous system development: what the knockouts are teaching us, Cell 77 (1994) 627–638.

[16] C. Crowley, S.D. Spencer, M.C. Nishimura, K.S. Chen, S. Pitts-Meek, M.P. Armanini, L.H. Ling, S.B. MacMahon, D.L. Shelton, A.D. Levinson, et al., Mice lacking nerve growth factor display perinatal loss of sensory and sympathetic neurons yet develop basal forebrain cholinergic neurons, Cell 76 (1994) 1001–1011.

[17] R.J. Smeyne, R. Klein, A. Schnapp, L.K. Long, S. Bryant, A. Lewin, S.A. Lira, M. Barbacid, Severe sensory and sympathetic neuropathies in mice carrying a disrupted Trk/NGF receptor gene, Nature 368 (1994) 246–249.

[18] A.M. Fagan, H. Zhang, S. Landis, R.J. Smeyne, I. Silos-Santiago, M. Barbacid, TrkA, but not TrkC, receptors are essential for survival of sympathetic neurons in vivo, J. Neurosci. 16 (1996) 6208–6218.

[19] A. Liu, M.S. Prenger, D.D. Norton, L. Mei, J.W. Kusiak, G. Bai, Nerve growth factor uses Ras/ERK and phosphatidylinositol 3-kinase cascades to up-regulate the *N*-methyl-D-aspartate receptor 1 promoter, J. Biol. Chem. 276 (2001) 45372–45379.

[20] I.N. Melnikova, P.D. Gardner, The signal transduction pathway underlying ion channel gene regulation by SP1-C-Jun interactions, J. Biol. Chem. 276 (2001) 19040–19045.

[21] E. Gizang-Ginsberg, E.B. Ziff, Nerve growth factor regulates tyrosine hydroxylase gene transcription through a nucleoprotein complex that contains c-Fos, Genes Dev. 4 (1990) 477–491.

[22] M. Ghee, H. Baker, J.C. Miller, E.B. Ziff, AP-1, CREB and CBP transcription factors differentially regulate the tyrosine hydroxylase gene, Mol. Brain Res. 55 (1998) 101–114.

[23] R. Katoh-Semba, S. Kitajima, Y. Yamazaki, M. Sano, Neuritic growth from a new subline of PC12 pheochromocytoma cells: cyclic AMP mimics the action of nerve growth factor, J. Neurosci. Res. 17 (1987) 36–44.

[24] T. Suzuki, T. Yamakuni, M. Hagiwara, H. Ichinose, Identification of ATF-2 as a transcriptional regulator for the tyrosine hydroxylase gene, J. Biol. Chem. 277 (2002) 40768–40774.

[25] P.C. Holm, F.J. Rodríguez, A. Kresse, J.M. Canals, I. Silos-Santiago, E. Arenas, Crucial role of TrkB ligands in the survival

and phenotypic differentiation of developing locus coeruleus noradrenergic neurons, Development 130 (2003) 3535–3545.
[26] Z. Guo, X. Du, L. Iacovitti, Regulation of tyrosine hydroxylase gene expression during transdifferentiation of striatal neurons: changes in transcription factors binding the AP-1 site, J. Neurosci. 18 (1998) 8163–8174.
[27] B. Sun, A.W. Tank, Overexpression of c-Fos is sufficient to stimulate tyrosine hydroxylase (TH) gene transcription in rat pheochromocytoma PC18 cells, J. Neurochem. 80 (2002) 295–306.
[28] B.B. Nankova, M. Rivkin, M. Kelz, E.J. Nestler, E.L. Sabban, Fos-related antigen 2: potential mediator of the transcriptional activation in rat adrenal medulla evoked by repeated immobilization stress, J. Neurosci. 20 (2000) 5647–5653.
[29] T. Nakajima, A. Fukamizu, J. Takahashi, F.H. Gage, T. Fisher, J. Blenis, M.R. Montminy, The signal-dependent coactivator CBP is a nuclear target for pp90RSK, Cell 86 (1996) 465–474.
[30] D.D. Ginty, A. Bonni, M.E. Greenberg, Nerve growth factor activates a Ras-dependent protein kinase that stimulates c-fos transcription via phosphorylation of CREB, Cell 77 (1994) 713–725.
[31] S. Ahn, M. Olive, S. Aggarwal, D. Krylov, D.D. Ginty, C. Vinson, A dominant-negative inhibitor of CREB reveals that it is a general mediator of stimulus-dependent transcription of c-fos, Mol. Cell. Biol. 18 (1998) 967–977.
[32] A. Riccio, S. Ahn, C.M. Davenport, J.A. Blendy, D.D. Ginty, Mediation by a CREB family transcription factor of NGF-dependent survival of sympathetic neurons, Science 286 (1999) 2358–2361.
[33] D.M. Ouwens, N.D. de Ruiter, G.C. van der Zon, A.P. Carter, J. Schouten, C. van der Burgt, K. Kooistra, J.L. Bos, J.A. Maassen, H. van Dam, Growth factors can activate ATF2 via a two-step mechanism: phosphorylation of Thr71 through the Ras-MEK-ERK pathway and of Thr69 through RalGDS-Src-p38, EMBO J. 21 (2002) 3782–3793.
[34] C. Trocmé, C. Sarkis, J.M. Hermel, R. Duchateau, S. Harrison, M. Simonneau, R. Al-Shawi, J. Mallet, CRE and TRE sequences of the rat tyrosine hydroxylase promoter are required for TH basal expression in adult mice but not in the embryo, Eur. J. Neurosci. 10 (1998) 508–521.
[35] J.W. Haycock, N.G. Ahn, M.H. Cobb, E.G. Krebs, ERK1 and ERK2, two microtubule-associated protein 2 kinases, mediate the phosphorylation of tyrosine hydroxylase at serine-31 in situ, Proc. Natl. Acad. Sci. USA 89 (1992) 2365–2369.
[36] N. Kaneda, T. Sasaoka, K. Kobayashi, K. Kiuchi, I. Nagatsu, Y. Kurosawa, K. Fujita, M. Yokoyama, T. Nomura, M. Katsuki, et al., Tissue-specific and high-level expression of the human tyrosine hydroxylase gene in transgenic mice, Neuron 6 (1991) 583–594.

Eur. J. Biochem. **271**, 349–355 (2004) © FEBS 2003 doi:10.1046/j.1432-1033.2003.03933.x

GTP cyclohydrolase I utilizes metal-free GTP as its substrate

Takahiro Suzuki[1,2], Hideki Kurita[3] and Hiroshi Ichinose[1,2]

[1]*Department of Life Science, Graduate School of Bioscience and Biotechnology, Tokyo Institute of Technology, Yokohama, Japan;* [2]*Division of Molecular Genetics, Institute for Comprehensive Medical Science;* [3]*Department of Hygiene, School of Medicine, Fujita Health University, Aichi, Japan*

GTP cyclohydrolase I (GCH) is the rate-limiting enzyme for the synthesis of tetrahydrobiopterin and its activity is important in the regulation of monoamine neurotransmitters such as dopamine, norepinephrine and serotonin. We have studied the action of divalent cations on the enzyme activity of purified recombinant human GCH expressed in *Escherichia coli*. First, we showed that the enzyme activity is dependent on the concentration of Mg-free GTP. Inhibition of the enzyme activity by Mg^{2+}, as well as by Mn^{2+}, Co^{2+} or Zn^{2+}, was due to the reduction of the availability of metal-free GTP substrate for the enzyme, when a divalent cation was present at a relatively high concentration with respect to GTP. We next examined the requirement of Zn^{2+} for enzyme activity by the use of a protein refolding assay, because the recombinant enzyme contained approximately one zinc atom per subunit of the decameric protein. Only when Zn^{2+} was present was the activity of the denatured enzyme effectively recovered by incubation with a chaperone protein. These are the first data demonstrating that GCH recognizes Mg-free GTP and requires Zn^{2+} for its catalytic activity. We suggest that the cellular concentration of divalent cations can modulate GCH activity, and thus tetrahydrobiopterin biosynthesis as well.

Keywords: GTP cyclohydrolase I; magnesium; recombinant protein; tetrahydrobiopterin; zinc.

Metal ions are essential for many physiological functions of the brain. They may also induce or aggravate numerous neurodegenerative processes. Thus, it is important to understand the roles of metal ions in normal and pathological brain functions.

GTP cyclohydrolase I (GCH) is the rate-limiting enzyme for the biosynthesis of tetrahydrobiopterin (BH_4), and the cellular BH_4 content is regulated mainly by the activity of this enzyme. BH_4 is an essential cofactor for three aromatic amino-acid monooxygenases – phenylalanine, tyrosine, and tryptophan hydroxylases – and for nitric oxide synthase [1]. BH_4 deficiency caused not only a decrease in the activity of these enzymes but also a decrease in the protein levels of tyrosine hydroxylase and nitric oxide synthase [2,3]. Therefore, the availability of BH_4 affects the amounts of neurotransmitters such as catecholamines, serotonin, melatonin and nitric oxide. The role of BH_4 in the activity of nitric oxide synthase also makes BH_4 an important factor for the immune system and endothelial cell function.

Various hormones and cytokines are known to induce the expression of the GCH gene in neural, lymphocytic and endothelial cells, and in different cell lines, resulting in an increased BH_4 content [4–8]. At the post-transcriptional level, BH_4 was shown to inhibit, and phenylalanine to stimulate, GCH activity through interaction with GFRP, a GTP cyclohydrolase I feedback regulatory protein [9]. GCH, which is a homodecameric protein, shows positive cooperativity against the GTP substrate [10] and phenylalanine changes the substrate velocity curve from sigmoidal to hyperbolic [11].

Recent biophysical studies suggest a stimulatory effect of Zn^{2+} [12] and Ca^{2+} [13] on GCH activity. By crystallographic analysis using purified *Escherichia coli* enzyme [14], an N-terminally truncated form of the recombinant human enzyme [12], and a stimulatory complex of rat GCH and GFRP induced by phenylalanine [15], Zn^{2+} was shown to be bound to the active centre of the homodecameric GCH enzyme. As for Ca^{2+}, mutations of the recombinant rat enzyme in an EF-hand-like motif, which is absent in bacteria, inhibited both the binding of Ca^{2+} to the enzyme and enzyme activity [13]. In addition, inhibition of the enzyme activity by various divalent cations including Mg^{2+} and Zn^{2+} was reported, based on experiments using crude preparations from mammalian and bacterial tissues [16] and the enzyme purified from rat liver [10].

In the present study, we examined the effect of various divalent cations on purified recombinant human GCH expressed in *E. coli* to clarify the molecular mechanism of action of divalent cations on the GCH enzymatic activity. We showed that GCH activity was totally dependent on metal-free GTP and that Mg^{2+} inhibited the enzyme activity by reducing the concentration of metal-free GTP by complex formation. Mg–GTP complex and Mg^{2+} had little effect on the GCH activity at the concentrations tested here. Also, by performing a protein refolding assay for GCH, we demonstrated that a stoichiometric amount of Zn^{2+} was

Correspondence to H. Ichinose, Department of Life Science, Graduate School of Bioscience and Biotechnology, Tokyo Institute of Technology, 4259, Nagatsuta-cho, Midori-ku, Yokohama 226-8501, Japan. Fax: + 81 45 924 5807, Tel.: + 81 45 924 5822, E-mail: hichinos@bio.titech.ac.jp

Abbreviations: BH_4, tetrahydrobiopterin; GCH, GTP cyclohydrolase I; GdnHCl, guanidine hydrochloride; NOS, nitric oxide synthase.

Enzyme: GTP cyclohydrolase I (EC 3.5.4.16).

(Received 4 September 2003, revised 11 November 2003, accepted 19 November 2003)

essential for the enzyme activity. Our data thus suggest that physiological and pathological changes in the levels of divalent cations including Mg^{2+} and Zn^{2+} may affect GCH activity and BH_4 levels *in vivo*.

Experimental procedures

Purification of recombinant human GCH

Recombinant human GCH was expressed in *E. coli* and purified as described previously [17]. We used this purified recombinant human enzyme for analysis of the action of divalent cations. Protein concentrations were determined by the method of Bradford [18], with bovine γ-globulin used as a standard.

Measurement of GCH activity

GCH activity was assayed as described previously [17]. The typical incubation mixture (total volume, 100 μL) contained 20 mM Tris/HCl (pH 7.5), 100 mM KCl, 1 $mg{\cdot}mL^{-1}$ BSA, and GTP as a substrate. The recombinant protein (10 μg) was incubated with various concentrations of GTP and divalent cations at 37 °C for 30 min.

Calculation of the concentrations of metal–GTP complex and metal-free GTP

Concentrations of metal-containing GTP, metal-free GTP, and GTP-free divalent cations in the reaction mixture for the measurement of the enzyme activity were determined by using the MAXCHELATOR program (WINMAXC ver.2.10 and SLIDERS ver.2.00, http://www.stanford.edu/~cpatton/maxc.html) [19]. Stability constants and enthalpy changes for metal–nucleotide complexes were obtained by referring to NIST Critically Selected Stability Constants of Metal Complexes: Version 6.0 (http://www.nist.gov/srd/nist46.htm). For calculation of concentrations of metal–GTP complex and metal-free GTP, we used stability constants and enthalpy changes of metal–ATP or proton–ATP complex as a substitute for those of the metal–GTP complex, because there were no data for stability constants and enthalpy changes of the Mg–, Zn–, Co– or Mn–GTP complexes in K^+ salt as a background electrolyte; however, stability constants of GTP with respect to Mg^{2+} in Na^+ salt as a background electrolyte and stability constants and enthalpy changes of GTP with respect to H^+ in K^+ salt as a background electrolyte were very similar to those of ATP in the database, and apparent stability constants of GTP with respect to Mg^{2+}, Mn^{2+} and Co^{2+} were almost the same as those of ATP given in a previous report [20]. Based on the condition of the incubation mixture for the enzyme activity described as above, parameters used in the calculation program were 37 °C, pH 7.5, and 0.110 ionic strength. Calculated values were considered to be accurate in a chelator-buffering range, which is within one order of magnitude of the K_d value for a metal–chelator complex.

Atomic absorption spectrophotometry

Zinc and calcium contents of the purified recombinant human GCH protein were determined by atomic absorption spectrophometry using a polarized Zeeman atomic absorption spectrometer, type Z-8100 (Hitachi, Tokyo, Japan).

Refolding assay

For the protein refolding assay in the presence of GroE, which is a chaperone protein, we referred to previous reports [21–24]. For denaturation, GCH was incubated on ice with 4 M guanidine hydrochloride (GdnHCl) for 30 min. The solution of denatured GCH was then diluted 100-fold with refolding buffer containing 50 mM Tris/HCl pH 7.5, 50 mM KCl, 1 mM dithiothreitol, 5 mM $MgCl_2$, 1 mM ATP, and a 2.5-fold molar excess of GroE. Equal molar amounts of GroES and GroEL (Takara Bio, Japan) were mixed for preparing the GroE complex. For refolding, the mixture was incubated at 25 °C for 60 min. Spontaneous refolding was performed in the absence of GroE.

For the experiment involving Zn^{2+} addition after refolding, the sample refolded in the presence of EGTA or Zn^{2+} was desalted by filtration through a spin-column (Micro Bio-spin 6, Bio-Rad). For elimination of Mg^{2+} and ATP, which are essential for the refolding reaction, as well as that of Zn^{2+} or EGTA, from the refolded samples, the spin-column was equilibrated with a solution containing 50 mM Tris/HCl pH 7.5, 50 mM KCl, and 1 mM dithiothreitol. After desalting, ions or chelators were added to aliquots of the filtered samples and preincubation was carried out at 25 °C for 5 min. Finally, aliquots of the samples (10 μL) were added to 90-μL volumes of the assay mixture for measurement of GCH activity, which was performed as described above.

Statistics

ANOVA followed by Bonferroni/Dunn's multiple comparison test was used for statistical evaluation of differences in the enzyme activity. $P < 0.05$ was accepted as statistically significant.

Results

Interaction of Mg^{2+} with the GTP substrate in solution is responsible for decrease in the GCH activity

GCH has enzyme activity in the absence of Mg^{2+}, whereas many other nucleotide hydrolyzing enzymes such as G proteins and kinases recognize Mg–GTP or Mg–ATP as the substrate. We first examined the effect of Mg^{2+} on the kinetics of enzyme activity of the purified recombinant human GCH. As shown in Fig. 1A, the dose–response curve for the GTP substrate was shifted to the right in the presence of 1 mM $MgCl_2$ and, to a much greater extent in the presence of 5 mM $MgCl_2$, whereas the enzyme activities at the high GTP concentrations remained unchanged. If Mg^{2+} acted directly on the enzyme we would expect the dose dependency of inhibition by $MgCl_2$ to be constant at various GTP concentrations. However, as shown in Fig. 1B, dose dependency for inhibition shifted to lower concentrations of $MgCl_2$ as the concentration of the GTP substrate was decreased. These results suggest that formation of the GTP–Mg^{2+} complex was responsible for the